Topological defects on fluctuating surfaces: General properties and the Kosterlitz-Thouless transition

Jeong-Man Park and T. C. Lubensky
Department of Physics, University of Pennsylvania, Philadelphia, Pennsylvania 19104
(Received 6 July 1995)

We investigate the Kosterlitz-Thouless transition for hexatic order on a free fluctuating membrane and derive both a Coulomb gas and a sine-Gordon Hamiltonian to describe it. The Coulomb-gas Hamiltonian includes charge densities arising from disclinations and from Gaussian curvature. There is an interaction coupling the difference between these two densities, whose strength is determined by the hexatic rigidity, and an interaction coupling Gaussian curvature densities arising from the Liouville Hamiltonian resulting from the imposition of a covariant cutoff. In the sine-Gordon Hamiltonian, there is a linear coupling between a scalar field and the Gaussian curvature. We discuss a gauge-invariant correlation function for hexatic order and the dielectric constant of the Coulomb gas. We also derive renormalization-group recursion relations that predict a transition with decreasing bending rigidity κ.

PACS number(s): 05.70.Jk, 68.10.−m, 87.22.Bt

I. INTRODUCTION

Bilayer fluid membranes [1,2] spontaneously self-assemble when aliphatic molecules are dissolved in water at a sufficiently high concentration. At high temperature, these membranes have no internal order and can be modeled as fluctuating structureless surfaces characterized by a bare bending rigidity κ. The bending rigidity is length-scale dependent and becomes zero at the persistence length $\xi_p = ae^{4\pi\kappa/3T}$, where a is a molecular length and T is the temperature. At length scales less than of order ξ_p, the membrane is flat; at longer length scales, it is crumpled.

A flat rigid membrane can have quasi-long-range (QLR) hexatic order [3] at low temperature and undergo a Kosterlitz-Thouless (KT) disclination unbinding transition [4–6] to a disordered high-temperature phase. A fluctuating membrane can also have QLR hexatic order [7]. Hexatic order stiffens the bending rigidity so that, rather than scaling to zero at long length scales, it approaches a constant times the hexatic rigidity K [8,9]. The hexatic membrane is thus more rigid than a fluid membrane, and it is said to be "crinkled" rather than crumpled. A fluctuating hexatic membrane can undergo a KT transition from the crinkled to the crumpled state. Reference [9] discusses two possible mechanisms for the crinkled-to-crumpled transition: disclination melting and crumpling. The latter mechanism is analogous to that producing the flat-to-crumpled transition in tethered membranes [10] and is argued to be associated with the buckling instability [11] of a membrane with a single disclination. Figure 1 shows a schematic phase-flow diagram in the $(\beta K)^{-1}$-$(\beta\kappa)^{-1}$ plane ($\beta = 1/T$) for a two-dimensional membrane embedded in three dimensions adapted from Ref. [9]. The vertical line at $(\beta K)^{-1} = \pi/72$ is the Kosterlitz-Thouless disclination unbinding line of a flat membrane. The curved line joining the vertical line at $(\beta\kappa)^{-1} = \pi/11$ is an estimate of the crumpling transition obtained by equating the energy of a single positive disclination in a buckled membrane to its entropy. Thus, the crumpling transition in this estimate is a Kosterlitz-Thouless transition in a buckled membrane. This schematic phase diagram describes qualitatively features that are in agreement with simple physical reasoning: for large κ, there should be a disclination melting to the crumpled phase as temperature is increased, and at fixed K, there should be a transition to the crumpled phase as κ is decreased. It, however, has features that are either unexpected or unexplained. The discontinuous change in curvature where the melting and crumpling lines join is surely an ar-

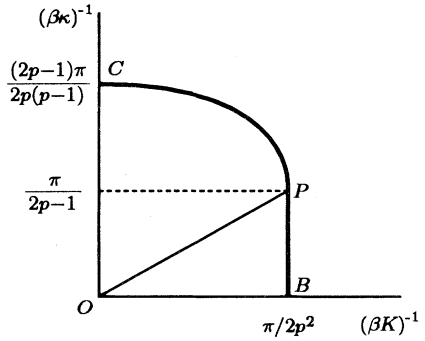

FIG. 1. Schematic phase diagram in the $(\beta K)^{-1}$-$(\beta\kappa)^{-1}$ plane adapted from [9]. The vertical line BP is the Kosterlitz-Thouless disclination melting line of a flat membrane. The curved line PC is an estimate of the crumpling critical line based upon a comparison of the energy and entropy of a single positive disclination in a buckled membrane. The line OP is the mechanical buckling instability line of a membrane with a single positive disclination. Above this line the zero-temperature membrane is buckled. Decreasing K or increasing T at fixed κ in the vicinity of P leads to a disclination melting transition to the crumpled phase. On decreasing κ at fixed K, the crumpled phase can only be reached by crossing the crumpling line.

tifact. It suggests that the physics of the crinkled-to-crumpled transition produced by decreasing K at fixed κ and by decreasing κ at fixed K are totally different, the latter being associated with the buckling instability of a membrane with a single disclination. It leaves unanswered whether the buckling instability line for the zero-temperature membrane has any significance for a membrane in thermal equilibrium, which is allowed to choose disclination configurations to minimize its free energy and thereby to reject highly energetic configurations with an excess of positive or negative disclinations.

In this paper, we present a detailed analysis of the low-temperature crinkled-to-crumpled transition in hexatic membranes. Our approach treats both disclinations and Gaussian curvature in the same real-space renormalization procedure and allows us to obtain recursion relations for κ, K, and the disclination fugacity y. Previous treatments used momentum space renormalization procedures to calculate the recursion relation for K and did not actually provide a complete set of recursion relations for κ, K, and y nor a prescription for doing so. Our procedure shows that thermally induced shape fluctuations cause a κ-dependent reduction in K, which to our knowledge is missed in previous calculation, that leads to the phase-flow diagram shown in Fig. 2. The vertical line in Fig. 1 is now curved, and the mechanism for

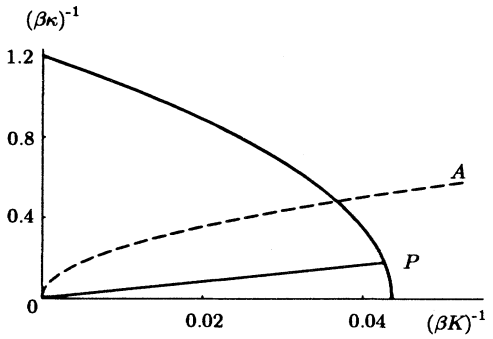

FIG. 2. Phase diagram for hexatic membranes ($p = 6$) in the $(\beta K)^{-1}$-$(\beta\kappa)^{-1}$ plane obtained from Eqs. (5.2), (5.3), and (5.7). The dark curved line [$(\beta K)^{-1} + (3/32\pi)(\beta\kappa)^{-2} = \pi/72 = 0.0436$] is the critical line separating the crinkled from the crumpled phase. The line OP is the crinkled line with $4(\beta\kappa)^{-1} = (\beta K)^{-1} + (3/32\pi)(\beta\kappa)^{-2}$]. P is the crinkled-to-crumpled fixed point. Unlike Fig. 1, the critical line has curvature at P. The dashed curve OA is the curve $2\pi(\beta K)^{-1} = (\beta\kappa)^{-2}$. The calculations in this paper are approximately valid in the region below this line where $(\beta\kappa)^{-1} < 1$ and $\beta K < 2\pi(\beta\kappa)^2$. The crinkled-to-crumpled transition occurs via disclination melting in the vicinity of P when either κ or K is decreased or when temperature is increased. Though our calculations do not apply above the curve OA, it plausible that the crumpled-to-crinkled transition occurs via disclination melting for all κ and K except at $K = \infty$, i.e., that the only effect of higher-order terms in $(\beta\kappa)^{-1}$ and $\beta K/(\beta\kappa)^2$ is to change the shape of the critical line. Alternatively, there could be some other phase boundary above the curve OA separating melting from some kind of crumpling transition.

the crinkled-to-crumpled phase transition in the vicinity of P, the termination of the crinkled line, is the same for decreasing both κ and K. Our renormalization equations allow us to study the fluid phase in the vicinity of the transition point P and to show that near P the persistance length is $\xi_{\rm KT}e^{4\pi\kappa/3T}$ rather than $ae^{4\pi\kappa/3T}$, where $\xi_{\rm KT} = a\exp(b/|T - T_{\rm KT}|^{1/2})$ is the KT correlation length (with b a constant), and $\bar{\kappa}$ is the bending rigidity at length scale $\xi_{\rm KT}$.

Our calculations are, strictly speaking, restricted to $(\beta\kappa)^{-1} < 1$, $(\beta K)^{-1} < 1$, and $(\beta K)/(\beta\kappa)^2 = TK/\kappa^2 < 1$, i.e., to the region below the curve OA in Fig. 2. We cannot, therefore, make any definitive statement about the interesting $K \to \infty$ limit, which should be related to the crumpling of tethered membranes. However, we believe that the phase diagram shown in Fig. 2 makes physical sense beyond the region of validity of our calculations. In this scenario, the transition from the crinkled to the crumpled phase would be controlled by the fixed point P in Fig. 2 for all $K^{-1} > 0$ and $\kappa^{-1} > 0$. The transition at $K = \infty$ would, however, be controlled by another fixed point.

We begin in Sec. II with a review of how to describe tangent plane order on fluctuating surfaces. We pay particular attention to correlation functions of orientational order. In order to compare tangent plane vectors at two different points on the surface, it is necessary to parallel transport one of the vectors along some path Γ to the position of the other vector. When Gaussian curvature is nonzero, the direction of a parallel transported vector depends on Γ even when there are no disclinations present. Physical correlation functions are invariant with respect to local coordinate transformations and for a particular membrane shape and distribution of disclinations depend on Γ. When correlation functions are averaged over shape and position of disclinations, the dependence on Γ vanishes.

In Sec. III, we discuss various models for hexatic membranes. We begin with the Hamiltonian for hexatic membranes expressed in terms of the orientational angle θ and a height variable. We then transform this model into a Coulomb-gas model in which "charge" density arises both from disclinations and from Gaussian curvature. There are two Coulomb-like terms in this Hamiltonian: one that is zero when the local disclination density equals the local Gaussian curvature and one, arising from the imposition of a covariant cutoff [12], that couples Gaussian curvature to Gaussian curvature. Finally, we transform the Coulomb-gas Hamiltonian to a sine-Gordon Hamiltonian with a term coupling the sine-Gordon field ϕ to the Gaussian curvature with an imaginary coefficient. The latter term is analogous to the dilaton coupling of string theory [13].

In Sec. IV, we relate the dielectric constant and hexatic rigidity to correlation functions of the disclination-Gaussian curvature density. We show in particular that the renormalized hexatic rigidity appearing in the orientational correlation function is the same as that calculated from the free energy. We also calculate the charge-density correlation functions.

Finally in Sec. V, we derive renormalization-group

(RG) recursion relations for K, κ, and the disclination fugacity y. These equations show that height fluctuations renormalize the hexatic rigidity in the absence of disclinations. This renormalized rigidity then flows under renormalization in the presence of disclination in exactly the same way as the rigidity of a flat membrane. If the initial height renormalized rigidity is less than the critical rigidity for a flat membrane, there is no rigid phase. Thus, height fluctuations can destroy the crinkled phase.

In Sec. VI, we review results and discuss some unanswered questions. In particular, we address the effect of asymmetry in the energies of positive and negative disclinations [14] on our results.

The focus of this paper is on the nature of tangent-plane order and the Kosterlitz-Thouless transition on fluctuating surfaces. It will not present a complete derivation of the RG equations used in Sec. V because they involve some two-loop graphs, which should be treated in a sophisticated regularization procedure. In a companion paper, [15] we derive the complete recursion relations from the sine-Gordon model using a real-space regularization procedure generalized from that used by Amit *et al.* [16] to treat the flat-space problem.

II. DIFFERENTIAL GEOMETRY AND TANGENT-PLANE ORDER

We are concerned with the nature of tangent-plane order on fluctuating membranes. In this section, we will review relevant concepts in differential geometry, mostly to establish notation. We will also discuss how to describe long-range order (or lack thereof) on a metric with fluctuating curvature.

A. Differential geometry of a plane

Points [17–19] on a two-dimensional surface embedded in three-dimensional Euclidean space are specified by a three-dimensional vector $\mathbf{R}(\mathbf{u})$ with components $R_i(\mathbf{u})$, $i = 1, 2, 3$, as a function of a two-dimensional parameter $\mathbf{u} = (u^1, u^2)$. Covariant tangent-plane vectors are then defined as

$$\mathbf{t}_\alpha = \partial_\alpha \mathbf{R}, \qquad \alpha = 1, 2, \tag{2.1}$$

where $\partial_\alpha = \partial/\partial u^\alpha$. We will use Greek letters $\alpha, \beta, \gamma, \ldots$ to denote components of covariant and contravariant tangent-plane tensors and Latin letters $i, j, k, \ldots$ to denote components of vectors and tensors in Euclidean space. The metric tensor is

$$g_{\alpha\beta} = \mathbf{t}_\alpha \cdot \mathbf{t}_\beta. \tag{2.2}$$

Its inverse $g^{\alpha\beta}$ satisfying

$$g^{\alpha\beta} g_{\beta\gamma} = \delta^\alpha_\gamma \tag{2.3}$$

allows us to define contravariant tangent-plane vectors $\mathbf{t}^\alpha = g^{\alpha\beta}\mathbf{t}_\beta$ satisfying $\mathbf{t}^\alpha \cdot \mathbf{t}_\beta = \delta^\alpha_\beta$. Any vector $\mathbf{V}$ in the tangent plane can be expressed as $\mathbf{V} = V^\alpha \mathbf{t}_\alpha = V_\alpha \mathbf{t}^\alpha$ where $V_\alpha = \mathbf{t}_\alpha \cdot \mathbf{V}$ and $V^\alpha = \mathbf{t}^\alpha \cdot \mathbf{V} = g^{\alpha\beta} V_\beta$ are, respectively, the covariant and contravariant components of $\mathbf{V}$. A unit normal $\mathbf{N}$ to the surface can be constructed from $\mathbf{t}_1$ and $\mathbf{t}_2$:

$$\mathbf{N} = \frac{\mathbf{t}_1 \times \mathbf{t}_2}{|\mathbf{t}_1 \times \mathbf{t}_2|}. \tag{2.4}$$

The curvature tensor is then

$$K_{\alpha\beta} = \mathbf{N} \cdot \partial_\alpha \partial_\beta \mathbf{R}. \tag{2.5}$$

From the curvature tensor, one can construct the mean curvature,

$$\frac{1}{2} H = \frac{1}{2} K^\alpha_\alpha = \frac{1}{2}\left(\frac{1}{R_1} + \frac{1}{R_2}\right), \tag{2.6}$$

and the Gaussian curvature,

$$S = \det K^\alpha_\beta = \frac{1}{R_1}\frac{1}{R_2}, \tag{2.7}$$

where R_1 and R_2 are the principal radii of curvature at the point of the surface in question. The integral of the Gaussian curvature is a topological invariant,

$$\int d^2u \sqrt{g} S = 4\pi(1 - \eta) = 2\pi\chi, \tag{2.8}$$

where η is the number of handles and $\chi = 2(1-\eta)$ is the Euler characteristic. In the Monge gauge, $\mathbf{u} = (x, y)$ and $\mathbf{R}(\mathbf{u}) = (\mathbf{u}, h(\mathbf{u}))$, and the metric tensor $g_{\alpha\beta}$ is written as

$$g_{\alpha\beta} = \partial_\alpha \mathbf{R} \cdot \partial_\beta \mathbf{R} = \begin{pmatrix} 1 + (\partial_x h)^2 & \partial_x h \partial_y h \\ \partial_x h \partial_y h & 1 + (\partial_x h)^2 \end{pmatrix}, \tag{2.9}$$

and the curvature tensor $K_{\alpha\beta}$ is

$$K_{\alpha\beta} = \mathbf{N} \cdot D_\alpha D_\beta \mathbf{R} = \frac{1}{\sqrt{1 + (\nabla h)^2}} \begin{pmatrix} \partial_x\partial_x h & \partial_x\partial_y h \\ \partial_y\partial_x h & \partial_y\partial_y h \end{pmatrix}, \tag{2.10}$$

where $(\nabla h)^2 = (\partial_x h)^2 + (\partial_y h)^2$.

The antisymmetric tensor $\gamma_{\alpha\beta}$ will be particularly useful in what follows. It is defined via

$$\begin{aligned} \gamma_{\alpha\beta} &= \mathbf{N} \cdot (\mathbf{t}_\alpha \times \mathbf{t}_\beta) \\ &= \frac{g_{\alpha 1} g_{\beta 2} - g_{\alpha 2} g_{\beta 1}}{|\mathbf{t}_1 \times \mathbf{t}_2|} \\ &= \sqrt{g}\,\epsilon_{\alpha\beta}, \end{aligned} \tag{2.11}$$

where $g = \det g_{\alpha\beta}$ and $\epsilon_{\alpha\beta}$ is the antisymmetric tensor with $\epsilon_{12} = -\epsilon_{21} = 1$. The contravariant tensor

$$\gamma^{\alpha\beta} = \mathbf{N} \cdot (\mathbf{t}^\alpha \times \mathbf{t}^\beta) \tag{2.12}$$

equals $\epsilon_{\alpha\beta}/\sqrt{g}$ and satisfies $\gamma^{\alpha\beta}\gamma_{\beta\alpha'} = -\delta^\alpha_{\alpha'}$. Finally the mixed tensor

$$\gamma^\alpha{}_\beta = g^{\alpha\alpha'}\gamma_{\alpha'\beta} \tag{2.13}$$

rotates vectors by $\pi/2$ since $V_\alpha \gamma^\alpha{}_\beta V^\beta = \gamma_{\alpha\beta} V^\alpha V^\beta = 0$ and $\gamma^\alpha{}_\beta V^\beta \gamma_\alpha{}^{\beta'} V_{\beta'} = V^\alpha V_\alpha$.

We are interested primarily in order in the tangent plane of unit (or fixed) magnitude. For this, it is useful to introduce orthonormal tangent-plane basis vectors $\mathbf{e}_1$ and $\mathbf{e}_2$ satisfying

$$\mathbf{e}_a \cdot \mathbf{e}_b = \delta_{ab}, \quad \mathbf{N} \cdot \mathbf{e}_a = 0. \tag{2.14}$$

A tangent vector $\mathbf{V}$ can be expressed in the basis $\{\mathbf{e}_1, \mathbf{e}_2\}$ as well as that defined by the covariant or contravariant vectors : $\mathbf{V} = V_a \mathbf{e}_a$ where $V_a = \mathbf{e}_a \cdot \mathbf{V}$. We will use Latin subscripts $a, b, c, \ldots$ to denote vector and tensor components with respect to the local orthonormal basis. Covariant derivatives are derivatives projected into the tangent plane. Components of the covariant derivative of a vector $\mathbf{V}$ relative to the orthonormal basis are

$$\begin{aligned} D_\alpha V_a &\equiv \mathbf{e}_a \cdot (\partial_\alpha \mathbf{V}) = \partial_\alpha V_a + \mathbf{e}_a \cdot \partial_\alpha \mathbf{e}_b V_b \\ &= \partial_\alpha V_a + \epsilon_{ab} A_\alpha V_b, \end{aligned} \tag{2.15}$$

where

$$A_\alpha = \mathbf{e}_1 \cdot \partial_\alpha \mathbf{e}_2 \tag{2.16}$$

is the spin-connection whose curl is the Gaussian curvature :

$$\gamma^{\alpha\beta} \partial_\alpha A_\beta = S. \tag{2.17}$$

We will also find it useful to use a circular basis defined by the vectors

$$\boldsymbol{\epsilon}_\pm = \frac{1}{\sqrt{2}} (\mathbf{e}_1 \pm i \mathbf{e}_2) = \boldsymbol{\epsilon}_\mp^*, \tag{2.18}$$

satisfying $\boldsymbol{\epsilon}_a \cdot \boldsymbol{\epsilon}_b^* = \delta_{ab}$ with $a, b = \pm$. In this basis, $\mathbf{V} = \tilde{V}_a \boldsymbol{\epsilon}_a^*$, and the covariant derivative,

$$\begin{aligned} D_\alpha \tilde{V}_\pm &= \boldsymbol{\epsilon}_\pm \cdot \partial_\alpha \mathbf{V} = \partial_\alpha \tilde{V}_\pm + \boldsymbol{\epsilon}_\pm \cdot \partial_\alpha \boldsymbol{\epsilon}_a^* V_a \\ &= \partial_\alpha \tilde{V}_\pm \mp i A_\alpha \tilde{V}_\pm \\ &= (\partial_\alpha \mp i A_\alpha) \tilde{V}_\pm, \end{aligned} \tag{2.19}$$

has a particularly simple form.

B. Vector and tensor order

A vector order parameter $\mathbf{S}$ that is restricted to lie in the tangent plane of a surface can be written as $S^\alpha \mathbf{t}_\alpha$ or $S_a \mathbf{e}_a$. If $\mathbf{S}$ is a unit length vector, it is conveniently expressed in terms of its angle in the local orthonormal basis as

$$\mathbf{S} = \cos\theta \mathbf{e}_1 + \sin\theta \mathbf{e}_2 = S_a \mathbf{e}_a, \tag{2.20}$$

where $S_1 = \cos\theta$ and $S_2 = \sin\theta$. The unit vector $\mathbf{S}$ can thus be written in the circular basis as

$$\mathbf{S} = \sqrt{2}\ \mathrm{Re}\ \boldsymbol{\Psi} \tag{2.21}$$

where

$$\boldsymbol{\Psi} = \psi \boldsymbol{\epsilon}_- \equiv e^{i\theta} \boldsymbol{\epsilon}_- \tag{2.22}$$

is a complex order parameter with unit length $\boldsymbol{\Psi} \cdot \boldsymbol{\Psi}^* = 1$.

We now turn to tensor tangent-plane order. The simplest nontrivial tensor order parameter is a symmetric-traceless tensor $\mathbf{Q}$ with Cartesian components

$$Q_{ij} = Q_{ab} e_{ai} e_{bj}. \tag{2.23}$$

The traceless constraint implies $Q_{ii} = Q_{aa} = 0$. $\mathbf{Q}$ is a uniaxial tensor with a principal axis lying along a unit vector $\mathbf{N} = n_a \mathbf{e}_a$ in the tangent plane. If we require that $\mathbf{Q}$ have a fixed magnitude defined by $\mathrm{Tr}\mathbf{Q}^2 = 1$, then we can write

$$Q_{ab} = \sqrt{2}(n_a n_b - \tfrac{1}{2}\delta_{ab}) \tag{2.24}$$

or

$$\begin{aligned} Q_{ij} = \frac{1}{\sqrt{2}} [&\cos(2\theta)(e_{1i}e_{1j} - e_{2i}e_{2j}) \\ &+ \sin(2\theta)(e_{1i}e_{2j} + e_{2i}e_{1j})]. \end{aligned} \tag{2.25}$$

This tensor, like the vector $\mathbf{S}$, can be expressed in terms of the real part of a complex tensor. We introduce the direct product tensor,

$$\boldsymbol{\Psi}_2 = \boldsymbol{\Psi} \otimes \boldsymbol{\Psi} = \psi_2 \boldsymbol{\epsilon}_- \otimes \boldsymbol{\epsilon}_- \equiv e^{2i\theta} \boldsymbol{\epsilon}_- \otimes \boldsymbol{\epsilon}_- , \tag{2.26}$$

with components $\Psi_{ij} = e^{2i\theta} \epsilon_{-i} \epsilon_{-j}$. Then

$$\mathbf{Q} = \sqrt{2}\ \mathrm{Re}\ \boldsymbol{\Psi}_2. \tag{2.27}$$

Generalization of this construction to higher-order tensors is straightforward. Let

$$\boldsymbol{\Psi}_p = \boldsymbol{\Psi} \otimes \cdots \otimes \boldsymbol{\Psi} = \psi_p \boldsymbol{\epsilon}_- \otimes \cdots \otimes \boldsymbol{\epsilon}_- , \tag{2.28}$$

with $\psi_p = e^{ip\theta}$ a pth-rank complex tangent-plane tensor. If we define the inner product of two tensors by

$$\boldsymbol{\Psi}_p \cdot \boldsymbol{\Phi}_p^* = \Psi_{i_1 \cdots i_p} \Phi^*_{i_1 \cdots i_p}, \quad \boldsymbol{\Psi}_p \cdot \boldsymbol{\Psi}_p^* = |\boldsymbol{\Psi}_p|^2 = 1, \tag{2.29}$$

then a real tensor, symmetric under interchanges of all indices and traceless with respect to all pairs of indices, is

$$\mathbf{Q}_p = \sqrt{2}\ \mathrm{Re}\ \boldsymbol{\Psi}_p. \tag{2.30}$$

The tensor $\boldsymbol{\Psi}_1 = \boldsymbol{\Psi}$ describes vector order such as is present in the smectic-C phase in which the long axes of molecules comprising the membrane tilt relative to the normal $\mathbf{N}$. $\boldsymbol{\Psi}_2$ describes tangent-plane nematic order with inversion symmetry. $\boldsymbol{\Psi}_6$ describes hexatic order. $\boldsymbol{\Psi}_4$ would describe "4-atic" order, etc. Thus $\boldsymbol{\Psi}_p$ for general p describes what we call "p-atic" order.

C. Tangent-plane correlations and parallel transport

In flat space, the basis vectors $\mathbf{e}_{1,2}$ or $\boldsymbol{\epsilon}_\pm$ are independent of spatial coordinate. Information about the existence of long-range order and about p-atic order parameter correlations is contained in the correlation function $\langle \boldsymbol{\Psi}_p(\mathbf{x}) \cdot \boldsymbol{\Psi}_p^*(\mathbf{x}') \rangle = \langle e^{-ip[\theta(\mathbf{x}') - \theta(\mathbf{x})]} \rangle$. Basis vectors at different points on curved surfaces are not identical (or even in the same plane) and the simple dot product of vec-

tors at different points does not carry information about tangent-plane order. In order to compare order parameters $\Psi_p(\mathbf{u})$ and $\Psi_p^*(\mathbf{u}')$ at two different points $\mathbf{u}$ and $\mathbf{u}'$, we need to parallel transport the order parameter at $\mathbf{u}$ along some path Γ to $\mathbf{u}'$. The parallel transported tensor $\Psi_p^\Gamma(\mathbf{u},\mathbf{u}')$ is now in the tangent plane at $\mathbf{u}'$ like $\Psi_p^*(\mathbf{u}')$ and we can take its dot product with $\Psi_p^*(\mathbf{u}')$. Thus the correlation function,

$$G_p(\mathbf{u},\mathbf{u}') = \langle \Psi_p(\mathbf{u}) : \Psi_p^*(\mathbf{u}')\rangle \equiv \langle \Psi_p^\Gamma(\mathbf{u},\mathbf{u}')\cdot\Psi_p^*(\mathbf{u}')\rangle, \tag{2.31}$$

where the ":" means parallel transported inner product, is what is appropriate for describing correlations in tangent-plane order. Note that this correlation function depends on the path Γ when the membrane has nonzero Gaussian curvature. We will find, however, that it becomes independent of Γ on nearly flat membranes after averaging over height fluctuations.

The parallel transported order parameter can be expressed in terms of the spin connection. Let $\mathbf{V}(\mathbf{u}) = V_a(\mathbf{u})\mathbf{e}_a(\mathbf{u})$ be a tangent vector at $\mathbf{u}$ and let $\mathbf{V}_a^{\parallel}(\mathbf{u}+\delta\mathbf{u}) = V_a^{\parallel}(\mathbf{u}+\delta\mathbf{u})\mathbf{e}_a(\mathbf{u}+\delta\mathbf{u})$ be the vector $\mathbf{V}(\mathbf{u})$ parallel transported to a nearby point $\mathbf{u}+\delta\mathbf{u}$. Then by definition $V_a^{\parallel}(\mathbf{u}+\delta\mathbf{u}) = V_a(\mathbf{u}) + \delta V_a(\mathbf{u})$ with

$$\delta V_a(\mathbf{u}) = -\epsilon_{ab}A_\alpha V_b(\mathbf{u})\delta u^\alpha. \tag{2.32}$$

Alternatively in terms of the circular basis,

$$\delta V_\pm(\mathbf{u}) = \pm iV_\pm(\mathbf{u})A_\alpha(\mathbf{u})\delta u^\alpha, \tag{2.33}$$

or

$$\tilde{V}_\pm^\Gamma(\mathbf{u},\mathbf{u}') = e^{\pm i\int_{\mathbf{u}}^{\mathbf{u}'} A_\alpha(\mathbf{u})du^\alpha}\tilde{V}_\pm(\mathbf{u}). \tag{2.34}$$

Applying this result to the vector $\Psi = \psi\epsilon_-$, we obtain

$$\Psi^\Gamma(\mathbf{u},\mathbf{u}') = e^{i\int_{\mathbf{u}}^{\mathbf{u}'} A_\alpha(\mathbf{u})du^\alpha}\Psi(\mathbf{u}), \tag{2.35}$$

or

$$\Psi^\Gamma(\mathbf{u},\mathbf{u}') = e^{i\int_{\mathbf{u}}^{\mathbf{u}'} A_\alpha(\mathbf{u})du^\alpha}e^{i\theta(\mathbf{u})}\epsilon_-(\mathbf{u}). \tag{2.36}$$

Thus we have

$$G_1(\mathbf{u},\mathbf{u}') = \left\langle e^{-i(\theta(\mathbf{u}')-\theta(\mathbf{u})-\int_{\mathbf{u}}^{\mathbf{u}'} A_\alpha(\mathbf{u})du^\alpha)}\right\rangle. \tag{2.37}$$

This function is invariant under changes in the local coordinate system (i.e., under nonlocal rotations of the vectors $\mathbf{e}_1$ and $\mathbf{e}_2$). The generalization to p-atic order is straightforward since by construction $\Psi_p(\mathbf{u}) : \Psi_p^*(\mathbf{u}') = [\Psi(\mathbf{u}) : \Psi^*(\mathbf{u}')]^p$ so that

$$G_p(\mathbf{u},\mathbf{u}') = \left\langle e^{-ip(\theta(\mathbf{u}')-\theta(\mathbf{u})-\int_{\mathbf{u}}^{\mathbf{u}'} A_\alpha(\mathbf{u})du^\alpha)}\right\rangle. \tag{2.38}$$

Again, this is invariant under coordinate system changes.

III. MODEL HAMILTONIANS

In this section, we will derive various equivalent representations for the Hamiltonian and associated partition function describing p-atic order on a fluctuating surface.

A. Fluid membranes

It is now well established that the long-wavelength properties of a fluid membrane are well described by the Helfrich-Canham Hamiltonian $\mathcal{H}_{\rm HC}$ [20,21,1], which can be expressed as a sum of three terms,

$$\mathcal{H}_{\rm HC} = \mathcal{H}_\kappa + \mathcal{H}_G + \mathcal{H}_\sigma. \tag{3.1}$$

The first term is the mean curvature energy,

$$\begin{aligned}\mathcal{H}_\kappa &= \frac{1}{2}\kappa\int d^2u\sqrt{g}H^2 \\ &= \frac{1}{2}\kappa\int d^2u\sqrt{g}\left(\boldsymbol{\nabla}\cdot\frac{\nabla h}{\sqrt{1+(\nabla h)^2}}\right)^2\end{aligned} \tag{3.2}$$

where $H = K_\alpha^\alpha$, and the second form is valid for the Monge gauge. The second term is the Gaussian curvature energy,

$$\mathcal{H}_G = \frac{1}{2}\kappa_G\int d^2u\sqrt{g}S, \tag{3.3}$$

where $S = \det K_\beta^\alpha$. This term is a topological invariant depending only on the genus of the surfaces. Since we will consider surfaces of fixed genus, we will drop this term. Finally

$$\mathcal{H}_\sigma = \sigma\int d^2u\sqrt{g} \tag{3.4}$$

is the surface tension energy. We are mostly interested in free membranes for which the renormalized surface tension obtained by differentiating the total free energy $\mathcal{F}$ with respect to the total surface area $\mathcal{A}$ ($\sigma_R = \partial\mathcal{F}/\partial\mathcal{A}$) is zero. Since there are entropic contributions to σ_R as well as contributions from internal order, the value of the bare surface tension σ will have to be adjusted to keep σ_R zero. In what follows, we will ignore $\mathcal{H}_\sigma$ with the understanding that it is really present if we want to keep track of how σ_R actually becomes zero.

The partition function for a fluid membrane,

$$\mathcal{Z}_{\rm fl} = \int \mathcal{D}\mathbf{R}(\mathbf{u})e^{-\beta\mathcal{H}_{\rm HC}} \tag{3.5}$$

is obtained by integrating over all physically distinct realizations of the surface, which is specified by the vector $\mathbf{R}(\mathbf{u})$. This means we have to specify a gauge or parametrization for $\mathbf{R}(\mathbf{u})$. Thus the measure $\mathcal{D}\mathbf{R}(\mathbf{u})$ for distinct surface configurations contains a Fadeev-Popov determinant [22]. In addition, it in general contains a factor to correct for the fact that different surface configurations arising from a fixed parametrization surface can have different areas [23].

B. p-atic order

As discussed in the preceding section, the complex tangent-plane tensor $\mathbf{\Psi}_p$ distinguishes a fluid membrane from one with p-atic tangent-plane order. Since $\mathbf{\Psi}_p$ has a fixed magnitude and there are no external fields aligning $\mathbf{\Psi}_p$ along a particular direction, the lowest nontrivial contribution to the energy associated with $\mathbf{\Psi}_p$ arises from its gradients,

$$\mathcal{H}_\theta = \frac{1}{2} K_p \int d^2u \sqrt{g} g^{\alpha\beta} D_\alpha \mathbf{\Psi}_p^* \cdot D_\beta \mathbf{\Psi}_p, \tag{3.6}$$

where D_α is a covariant derivative. Using Eq. (2.19) and Eq. (2.28), it is straightforward to show

$$D_\alpha \mathbf{\Psi}_p = ip(\partial_\alpha \theta - A_\alpha)\mathbf{\Psi}_p \tag{3.7}$$

and

$$\mathcal{H}_\theta = \frac{1}{2} K \int d^2u \sqrt{g} g^{\alpha\beta} (\partial_\alpha \theta - A_\alpha)(\partial_\beta \theta - A_\beta), \tag{3.8}$$

where we set $K = K_p p^2$. Equation (3.8) is the simplest energy arising from p-atic order. It is rotationally isotropic, and it describes correctly the lowest-order gradient contribution to the energy for all $p \geq 3$. For $p = 1$ or $p = 2$, however, this energy should have anisotropic contributions [24,25]. In this paper, we ignore these anisotropies.

The p-atic order parameter $\mathbf{\Psi}_p$ can have disclinations of strength $q = 2\pi(k/p)$ where k is an integer [26]. A disclination at $\mathbf{u} = \mathbf{u}_\nu$ with strength q_ν gives rise to a singular contribution θ^{sing} to θ satisfying

$$\oint_\Gamma du^\alpha \partial_\alpha \theta^{\text{sing}} = q_\nu, \tag{3.9}$$

where Γ is a contour enclosing $\mathbf{u}_\nu$. Thus, in general $\partial_\alpha \theta = \partial_\alpha \theta' + v_\alpha$ where θ' is nonsingular, $v_\alpha = \partial_\alpha \theta^{\text{sing}}$, and

$$\gamma^{\alpha\beta} \partial_\alpha v_\beta = n(\mathbf{u}), \tag{3.10}$$

where

$$n(\mathbf{u}) = \frac{1}{\sqrt{g}} \sum_\nu q_\nu \delta(\mathbf{u} - \mathbf{u}_\nu) \tag{3.11}$$

is the disclination density. The vector v_α can always be chosen so that it is purely transverse, so that $D_\alpha v^\alpha = 0$. In the p-atic Hamiltonian, $\partial_\alpha \theta$ always occurs in the combination $\partial_\alpha \theta - A_\alpha$. The spin-connection A_α can and will in general have both a longitudinal and a transverse component. However, one can always redefine θ' to include the longitudinal part of A_α. This amounts to choosing locally rotated orthonormal vectors $\mathbf{e}_1(\mathbf{u})$ and $\mathbf{e}_2(\mathbf{u})$ so that $D_\alpha A^\alpha = 0$. Thus we may take both v_α and A_α to be transverse and the p-atic Hamiltonian,

$$\begin{aligned} \mathcal{H}_\theta &= \frac{1}{2} K \int d^2u \sqrt{g} g^{\alpha\beta} (\partial_\alpha \theta' + v_\alpha - A_\alpha) \\ &\quad \times (\partial_\beta \theta' + v_\beta - A_\beta) \\ &= \mathcal{H}_\parallel + \mathcal{H}_\perp, \end{aligned} \tag{3.12}$$

can be decomposed into a regular longitudinal part,

$$\mathcal{H}_\parallel = \frac{1}{2} K \int d^2u \sqrt{g} g^{\alpha\beta} \partial_\alpha \theta' \partial_\beta \theta', \tag{3.13}$$

and a transverse part,

$$\mathcal{H}_\perp = \frac{1}{2} K \int d^2u \sqrt{g} g^{\alpha\beta} (v_\alpha - A_\alpha)(v_\beta - A_\beta), \tag{3.14}$$

where it is understood that $D_\alpha(v^\alpha - A^\alpha) = 0$.

It costs an energy $\epsilon_c(k)$ to create the core of a disclination of strength k. (We assume for the moment that the core energies of the positive and negative disclinations are the same. See, however, Ref. [14] and the summary section.) Thus, partition sums should be weighted by a factor $y_k = e^{-\beta \epsilon_c(k)}$ for each disclination of strength k. Since $\epsilon_c(k) \sim k^2$, we may at low temperature restrict our attention to configurations in which only configurations of strength ± 1 appear. Let $N_\pm$ be the number of disclinations of strength ± 1 and let $\mathbf{u}_{\nu^\pm}$ be the coordinate of the core of the disclination with strength ± 1 labeled by ν. The p-atic membrane partition function can then be written as

$$\mathcal{Z}(\kappa, K, y) = \text{Tr}_v y^N \int \mathcal{D}\mathbf{R} \int \mathcal{D}\theta e^{-\beta \mathcal{H}_\kappa} e^{-\beta \mathcal{H}_\theta}, \tag{3.15}$$

where $y = y_1$, and $N = N_+ + N_-$. $\mathcal{H}_\theta$ depends on all of the disclination coordinates $\mathbf{u}_{\nu^\pm}$ where $\nu^\pm = 1, 2, \ldots, N_\pm$, and

$$\begin{aligned} \text{Tr}_v = &\sum_{N_+, N_-} \delta_{N_+ + N_-, p\chi} \frac{1}{N_+! N_-!} \\ &\times \prod_{\nu^+} \int \frac{d^2u_{\nu^+}}{a^2} \prod_{\nu^-} \int \frac{d^2u_{\nu^-}}{a^2}, \end{aligned} \tag{3.16}$$

where a is a molecular length. The Kronecker factor $\delta_{N_+ + N_-, p\chi}$ in Tr_v imposes the topological constraint [27] that the total disclination strength on a surface with Euler characteristic χ be equal to χ. Thus, on a sphere with $\chi = 2$, $N_+ + N_- = 2p$. If $p = 6$, for example, there must be 12 more positive than negative disclinations. On a nearly flat surface, the Coulomb interaction effectively restricts N_+ to equal N_-, and we use Eq. (3.16) with $\chi = 0$ even though χ for an open surface is, strictly speaking, equal to 1 [28].

C. The Coulomb-gas model

The p-atic model of Eq. (3.15) can easily be converted to a Coulomb-gas model using

$$\gamma^{\alpha\beta} \partial_\alpha (v_\beta - A_\beta) = n - S \equiv \rho, \tag{3.17}$$

which follows from Eq. (2.17) and Eq. (3.10). The quantity $\rho = n - S$ is a "charge" density with contributions arising both from disclinations and Gaussian curvature. Equation (3.17) implies

$$v_\alpha - A_\alpha = -\gamma_\alpha{}^\beta D_\beta \frac{1}{\Delta_g} \rho, \tag{3.18}$$

where $\Delta_g = D^\alpha D_\alpha = (1/\sqrt{g})\partial_\alpha \sqrt{g} g^{\alpha\beta}\partial_\beta$ is the Laplacian on a surface with metric tensor $g_{\alpha\beta}$ acting on a scalar. Recall [Eq. (2.13)] that $\gamma_\alpha{}^\beta$ rotates a vector by $\pi/2$ so that $v_\alpha - A_\alpha$ is perpendicular to $D_\beta(-\Delta_g)^{-1}\rho$ and is thus manifestly transverse. Using Eq. (3.18) in Eq. (3.14), we obtain

$$\mathcal{Z} = \mathrm{Tr}_v y^N \int \mathcal{D}\mathbf{R} \int \mathcal{D}\theta' e^{-\beta\mathcal{H}_\kappa - \beta\mathcal{H}_\parallel - \beta\mathcal{H}_c}, \tag{3.19}$$

where

$$\mathcal{H}_c = \frac{1}{2}K \int d^2u d^2u' \sqrt{g}\rho(\mathbf{u}) \left(-\frac{1}{\Delta_g}\right)_{\mathbf{u}\mathbf{u}'} \sqrt{g'}\rho(\mathbf{u}') \tag{3.20}$$

is the Coulomb Hamiltonian associated with the charge ρ. The longitudinal variable θ' appears only quadratically in $\mathcal{H}_\parallel$ and the trace over θ' can be done directly:

$$\int \mathcal{D}\theta' e^{-\beta\mathcal{H}_\parallel} = e^{-\beta\mathcal{H}_L}, \tag{3.21}$$

where

$$\beta\mathcal{H}_L = \frac{1}{8\pi a^2}\int d^2u\sqrt{g} - \frac{1}{24\pi}\int d^2u d^2u'\sqrt{g}S(\mathbf{u}) \times \left(-\frac{1}{\Delta_g}\right)_{\mathbf{u}\mathbf{u}'} \sqrt{g'}S(\mathbf{u}') \tag{3.22}$$

is the Liouville action [12,19] arising from the conformal anomaly. The first term in this expression is proportional to the surface area and can be incorporated into the surface tension energy $\mathcal{H}_\sigma$ by shifting the surface tension σ. We assume, as discussed earlier, that the total surface tension is zero. We will, therefore, ignore this term in what follows. The second term can be viewed as a Coulomb interaction for Gaussian curvature but with a negative coupling constant, i.e., an imaginary charge.

The Coulomb-gas partition function can thus be written as

$$\begin{aligned}\mathcal{Z} &= \mathrm{Tr}_v y^N \int \mathcal{D}\mathbf{R} e^{-\beta\mathcal{H}_\kappa - \beta\mathcal{H}_L - \beta\mathcal{H}_C} \\ &= \mathrm{Tr}_v y^N \int \mathcal{D}\mathbf{R} e^{-\beta\mathcal{H}_\kappa - \beta\mathcal{H}_{\mathrm{CT}}},\end{aligned} \tag{3.23}$$

where

$$\begin{aligned}\mathcal{H}_{\mathrm{CT}} &= \frac{1}{2}K\int d^2u d^2u'\sqrt{g}\rho(\mathbf{u})\left(-\frac{1}{\Delta_g}\right)_{\mathbf{u}\mathbf{u}'}\sqrt{g'}\rho(\mathbf{u}') \\ &\quad -\frac{T}{24\pi}\int d^2u d^2u'\sqrt{g}S(\mathbf{u})\left(-\frac{1}{\Delta_g}\right)_{\mathbf{u}\mathbf{u}'}\sqrt{g'}S(\mathbf{u}') \\ &= \frac{1}{2}K'\int d^2u d^2u'\sqrt{g}S(\mathbf{u})\left(-\frac{1}{\Delta_g}\right)_{\mathbf{u}\mathbf{u}'}\sqrt{g'}S(\mathbf{u}') \\ &\quad +\frac{1}{2}K\int d^2u d^2u'\sqrt{g}n(\mathbf{u})\left(-\frac{1}{\Delta_g}\right)_{\mathbf{u}\mathbf{u}'}\sqrt{g'}n(\mathbf{u}') \\ &\quad -K\int d^2u d^2u'\sqrt{g}n(\mathbf{u})\left(-\frac{1}{\Delta_g}\right)_{\mathbf{u}\mathbf{u}'}\sqrt{g'}S(\mathbf{u}') \\ &\equiv \mathcal{H}_{SS} + \mathcal{H}_{nn} + \mathcal{H}_{nS}\end{aligned} \tag{3.24}$$

is the "total" Coulomb Hamiltonian in which there are two distinct charge densities, ρ and S, or, equivalently, n and S. The coupling constant for Gaussian curvature interactions in the absence of disclinations is

$$K' = K - T/12\pi. \tag{3.25}$$

This is the shifted coupling arising from the Liouville term discussed in Refs. [8] and [9]. The coupling constants for disclinations and between disclinations and Gaussian curvature are not shifted by the Liouville term and remain equal to K.

D. The sine-Gordon model

The Coulomb-gas model can be converted following standard procedures into a sine-Gordon model. The first step is to carry out a Hubbard-Stratonovich transformation on $\beta\mathcal{H}_C$:

$$e^{-\beta\mathcal{H}_C} = e^{\beta\mathcal{H}_L}\int \mathcal{D}\phi e^{-1/(2\beta K)\int d^2u\sqrt{g}\partial^\alpha\phi\partial_\alpha\phi} e^{i\int d^2u\sqrt{g}\rho\phi}, \tag{3.26}$$

where the Liouville factor $e^{\beta\mathcal{H}_L}$ is needed to ensure that $e^{-\beta\mathcal{H}_C}$ be one when $\rho = 0$. Inserting this in Eq. (3.23), we obtain

$$\mathcal{Z} = \mathrm{Tr}_v y^N \int \mathcal{D}\mathbf{R}\mathcal{D}\phi e^{-\beta\mathcal{H}_\kappa} e^{-\beta\mathcal{H}_\phi} e^{i\int d^2u\sqrt{g}(n-S)\phi}, \tag{3.27}$$

where

$$\beta\mathcal{H}_\phi = \frac{1}{2\beta K}\int d^2u\sqrt{g}\partial^\alpha\phi\partial_\alpha\phi. \tag{3.28}$$

The only dependence on disclinations is now in the term linear in n. Thus to carry out Tr_v, we need only to evaluate

$$\begin{aligned}\mathrm{Tr}_v y^N e^{i\int d^2u\sqrt{g}n} &= \sum_{N_+,N_-}\frac{1}{N_+!N_-!}\delta_{N_+-N_-,p\chi}y^{N_++N_-}\left(\int\frac{d^2u\sqrt{g}}{a^2}e^{2\pi i\phi(\mathbf{u})/p}\right)^{N_+}\left(\int\frac{d^2u\sqrt{g}}{a^2}e^{-2\pi i\phi(\mathbf{u})/p}\right)^{N_-} \\ &= \sum_{N_+,N_-}\frac{1}{N_+!N_-!}\int\frac{d\omega}{2\pi}e^{i\omega p\chi}\left(y\int\frac{d^2u\sqrt{g}}{a^2}e^{i\{2\pi[\phi(\mathbf{u})/p]-\omega\}}\right)^{N_+}\left(y\int\frac{d^2u\sqrt{g}}{a^2}e^{-i\{2\pi[\phi(\mathbf{u})/p]-\omega\}}\right)^{N_-} \\ &= \int\frac{d\omega}{2\pi}e^{i\omega p\chi}e^{(2y/a^2)\int d^2u\sqrt{g}\cos[2\pi(\phi/p)-\omega]}.\end{aligned} \tag{3.29}$$

Thus

$$\mathcal{Z} = \int \frac{d\omega}{2\pi} \int \mathcal{D}\phi \int \mathcal{D}\mathbf{R} e^{-\beta\mathcal{H}_\kappa} e^{-\beta\mathcal{H}_\phi} e^{i\omega p\chi} e^{(2y/a^2)\int d^2u\sqrt{g}\cos[2\pi(\phi/p)-\omega]} e^{-i\int d^2u\sqrt{g}S\phi}. \tag{3.30}$$

We can now change variables, letting $\phi = (p/2\pi)(\phi' + \omega)$. The term linear in the Gaussian curvature then becomes

$$-i\int d^2u\sqrt{g}S\frac{p}{2\pi}(\omega+\phi') = -i\omega p\chi - i\frac{p}{2\pi}\int d^2u\sqrt{g}S\phi', \tag{3.31}$$

where we used Eq. (2.8) relating χ to the integral of the Gaussian curvature. Thus the ω-dependent part of this term exactly cancels the $i\omega p\chi$ term arising from the integral representation of the Kronecker δ function. The integral over ω in Eq. (3.30) is now trivial, and we obtain

$$\mathcal{Z} = \int \mathcal{D}\phi \int \mathcal{D}\mathbf{R} e^{-\beta\mathcal{H}_\kappa} e^{-\mathcal{L}}, \tag{3.32}$$

where

$$\mathcal{L} = \frac{1}{2\beta K}\left(\frac{p}{2\pi}\right)^2 \int d^2u\sqrt{g}g^{\alpha\beta}\partial_\alpha\phi\partial_\beta\phi - \frac{2y}{a^2}\int d^2u\sqrt{g}\cos\phi - i\frac{p}{2\pi}\int d^2u\sqrt{g}S\phi \tag{3.33}$$

is the sine-Gordon action on a fluctuating surface of arbitrary genus. The first two terms of this action are the gradient and cosine energies present in a flat space. The final term provides the principal coupling between ϕ and fluctuations in the metric. It is analogous to the dilaton coupling [13] of string theory though here the coupling constant is imaginary rather than real. Note that the Liouville action is not explicitly present in Eq. (3.32). The requirement that the cutoff ϕ be applied in a covariant fashion is, however, still present. Thus, if $g = 0$, the integral over ϕ will yield the Liouville factor. When y is not zero, care must be taken to implement any cutoffs in integrals in a covariant fashion.

IV. THE DIELECTRIC CONSTANT AND HEXATIC RIGIDITY

In the preceding section, we derived several equivalent expressions for the partition function of a fluctuating membrane with internal p-atic order. In this section, we will derive an expression for the inverse dielectric constant associated with the charge density ρ and show that it is equivalent to the renormalized p-atic rigidity controlling the gauge-invariant p-atic correlation function of Eq. (2.31). We will begin by reviewing the derivation of the longitudinal dielectric constant in flat space. We will then derive the dielectric constant and renormalized rigidities on fluctuating surfaces.

A. Flat-space dielectric constant

Consider a system with an internal charge density ρ and fixed or controllable external charge density ρ_e. To be concrete, ρ_e could be the free charge at the metal electrodes of a capacitor. The total charge density is $\rho_T = \rho + \rho_e$. The electric field $\mathcal{E}$ is determined by the total charge:

$$\nabla\cdot\mathcal{E} = \alpha\rho_T. \tag{4.1}$$

Here α sets the units of charge (for example, $\alpha = \epsilon_0^{-1}$ in mks units). The displacement vector $\mathcal{D} = \epsilon\alpha^{-1}\mathcal{E}$, where ϵ is the dielectric constant, is controlled by the external charge:

$$\nabla\cdot\mathcal{D} = \nabla\cdot\mathcal{D}_\parallel = \rho_e, \tag{4.2}$$

where $\mathcal{D}_\parallel$ is the longitudinal part of $\mathcal{D}$. The electric potential can be introduced in the usual way: $\mathcal{E} = -\nabla\phi_T$, $\mathcal{D}_\parallel = -\alpha^{-1}\nabla\phi_e$, and $\phi_T = \phi + \phi_e$, where $-\nabla^2\phi = \alpha\rho$ and $-\nabla^2\phi_e = \alpha\rho_e$.

The inverse longitudinal dielectric constant is obtained by expanding the free energy to second order in $\mathcal{D}_\parallel = -\nabla\phi_e$:

$$\Delta\mathcal{F} = \frac{1}{2}\alpha^{-1}\int d^dx d^dx' \epsilon_\parallel^{-1}(\mathbf{x},\mathbf{x}')\nabla\phi_e(\mathbf{x})\cdot\nabla\phi_e(\mathbf{x}'). \tag{4.3}$$

A wave-number-dependent dielectric constant can be obtained if $\epsilon_\parallel^{-1}(\mathbf{x},\mathbf{x}')$ is translationally invariant or by carrying out the usual Maxwell averaging procedure. The result is

$$\epsilon_\parallel^{-1}(\mathbf{q}) = \frac{1}{q^2}\left(\frac{\alpha}{V}\right)\int d^dx d^dx' e^{-i\mathbf{q}\cdot(\mathbf{x}-\mathbf{x}')}\frac{\delta^2\mathcal{F}}{\delta\phi_e(\mathbf{x})\delta\phi_e(\mathbf{x}')}, \tag{4.4}$$

where $V = \int d^dx$ is the volume of the system. We can use this formula to relate $\epsilon_\parallel^{-1}(\mathbf{q})$ to correlations of the charge density. The Coulomb Hamiltonian can be written as

$$\begin{aligned}\mathcal{H}_C &= \frac{1}{2}\alpha\int d^dx d^dx' \rho_T(\mathbf{x})\left(-\frac{1}{\nabla^2}\right)_{\mathbf{x}\mathbf{x}'}\rho_T(\mathbf{x}') \\ &= \frac{1}{2}\alpha^{-1}\int d^dx(\nabla\phi_e)^2 + \frac{1}{2}\int d^dx\rho\phi \\ &\quad + \int d^dx\rho\phi_e.\end{aligned} \tag{4.5}$$

Expanding $\mathcal{F} = -T\ln e^{-\beta(\mathcal{H}_0+\mathcal{H}_C)}$, where $\mathcal{H}_0$ is the non-Coulombic contribution to the Hamiltonian to second order in $\nabla\phi_e$, we obtain

$$\Delta\mathcal{F} = \frac{1}{2}\alpha^{-1}\int d^dx(\nabla\phi_e)^2 - \frac{1}{2}\beta\int d^dx\phi_e(\mathbf{x})\phi_e(\mathbf{x}')\langle\rho(\mathbf{x})\rho(\mathbf{x}')\rangle \tag{4.6}$$

and

$$\epsilon_{\parallel}^{-1}(\mathbf{q}) = 1 - \frac{\beta\alpha}{q^2} C_{\rho\rho}(\mathbf{q}), \tag{4.7}$$

where

$$C_{\rho\rho}(\mathbf{q}) = \frac{1}{V}\int d^d x d^d x' e^{-i\mathbf{q}\cdot(\mathbf{x}-\mathbf{x}')}\langle\rho(\mathbf{x})\rho(\mathbf{x}')\rangle \tag{4.8}$$

is the density correlation function. Equation (4.7) is the well-known expression [31] relating ϵ^{-1} to the charge susceptibility $\chi_{\rho\rho} = \beta C_{\rho\rho}$. In what follows, we will use the notation introduced in Eq. (4.8) for arbitrary variables,

$$C_{AB}(\mathbf{q}) = \frac{1}{A_B}\int d^2 x d^2 x' e^{-i\mathbf{q}\cdot(\mathbf{x}-\mathbf{x}')}\langle A(\mathbf{x})B(\mathbf{x}')\rangle, \tag{4.9}$$

where we have set $d = 2$ and $V = A_B$.

B. Dielectric constant on a fluctuating membrane

We can now determine the dielectric constant associated with the charge $\rho = n - S$ on a fluctuating membrane following exactly the procedures outlined in the preceding subsection. We impose external charges ρ_e to create a constant slowly varying external potential ϕ_e. These charges lead to a total charge density $\rho_T = \rho + \rho_e$. They should not, however, change the Gaussian curvature because otherwise they would change the Liouville energy. Thus ρ_e must arise from disclinations that we can, for concreteness, place at the boundary of the membrane like the charge on capacitor electrodes. In analogy with flat space, we can introduce external and induced electric potentials ϕ_e and ϕ satisfy $-\Delta_g\phi = \rho$ and $-\Delta_g\phi_e = \rho_e$ with $\phi_T = \phi + \phi_e$ the total potential. The Coulomb Hamiltonian can then be written as

$$\mathcal{H}_C = \frac{1}{2}K^{-1}\int d^2u\sqrt{g}g^{\alpha\beta}\partial_\alpha\phi_e\partial_\beta\phi_e + \frac{1}{2}\int d^2u\sqrt{g}\rho\phi + \int d^2u\sqrt{g}\rho\phi_e. \tag{4.10}$$

We are interested in the long-wavelength dielectric constant for our presumed macroscopically flat (or nearly flat) membrane. For this purpose it is most convenient to use the Monge gauge in which $\mathbf{u} = \mathbf{x} \equiv (x, y)$ measures position in the average plane of the membrane. In this case $\phi_e(\mathbf{u}) \to \phi_e(\mathbf{x})$ is a slowly varying function of $\mathbf{x}$, which, in the limit of fixed charge density at membrane boundaries, grows linearly with $\mathbf{x}$. The long-wavelength dielectric constant for our nearly flat membrane can be obtained using Eq. (4.4), where $\mathbf{q}$ is the Fourier variable dual to position $\mathbf{x}$, and Eq. (4.9) for $\mathcal{H}_C$. Using Eq. (4.9) and expanding $\mathcal{F}$ to second order in ϕ_e, we obtain

$$\Delta\mathcal{F} = \frac{1}{2}K^{-1}\int d^2u\langle\sqrt{g}g^{\alpha\beta}\partial_\alpha\phi_e\partial_\beta\phi_e\rangle - \frac{1}{2}\beta\int d^2u\int d^2u'\langle\sqrt{g}\rho(\mathbf{x})\sqrt{g'}\rho(\mathbf{x}')\rangle\phi_e(\mathbf{x})\phi_e(\mathbf{x}') \tag{4.11}$$

and

$$\epsilon_{\parallel}^{-1}(\mathbf{q}) = \frac{q_\alpha q_\beta}{q^2}\langle\sqrt{g}g^{\alpha\beta}\rangle - \frac{\beta K}{q^2}C_{\tilde{\rho}\tilde{\rho}}(\mathbf{q}) \tag{4.12}$$

is the charge-density correlation function for

$$\tilde{\rho} = \sqrt{g}\rho\ , \tag{4.13}$$

rather than ρ. $\tilde{\rho}$ is in fact the effective charge density for the coarse-grained flat surface (with metric tensor equal to unity) because the total charge in an area patch d^2x should not change under coarse graining. The quantity $\langle\sqrt{g}g^{\alpha\beta}\rangle$ is equal to $\delta^{\alpha\beta}$ as can be verified easily to lowest order in T in the Monge gauge or more generally using the conformal gauge [29,30]. Thus we have

$$\epsilon_{\parallel}^{-1}(\mathbf{q}) = 1 - \frac{\beta K}{q^2}C_{\tilde{\rho}\tilde{\rho}}(\mathbf{q}). \tag{4.14}$$

$C_{\tilde{\rho}\tilde{\rho}}(\mathbf{q})$ is the charge-density correlation function evaluated in the presence of all interactions, including the Coulomb-like $\mathcal{H}_L$. We will return at the end of this section to its evaluation.

C. Hexatic rigidity

In this section we will show that the renormalized hexatic rigidity K_R is equal to $\alpha\epsilon_{\parallel}^{-1}$. To calculate K_R, we introduce a shift ω_α in $\partial_\alpha\theta'$ via $\partial_\alpha\theta' \to \partial_\alpha\theta' + \omega_\alpha$ in Eq. (3.13) and evaluate the free energy to second order in ω_α. Using Eq. (4.11), we obtain

$$\Delta\mathcal{F} = \frac{1}{2}K\int d^2u\langle\sqrt{g}g^{\alpha\beta}\omega_\alpha\omega_\beta\rangle - \frac{1}{2}\beta K^2\int d^2u\int d^2u'\langle\sqrt{g}D^\alpha\theta'\sqrt{g'}D^\beta\theta'\omega_\alpha\omega_\beta\rangle - \frac{1}{2}\beta K^2\int d^2u\int d^2u'\langle\sqrt{g}(v^\alpha - A^\alpha)\sqrt{g'}(v^\beta - A^\beta)\omega_\alpha\omega_\beta\rangle. \tag{4.15}$$

As discussed previously, θ' decouples from other variables. For any given realization of the surface $\langle\theta\theta'\rangle = (T/K)(-\Delta_g^{-1})$. We can therefore combine the first two terms in Eq. (4.15) to obtain

$$\Delta\mathcal{F} = \frac{1}{2}K\int d^2u d^2u'\langle\sqrt{g}\omega_\alpha\mathcal{P}_\perp^{\alpha\beta}\sqrt{g'}\omega_\beta\rangle - \frac{1}{2}\beta K^2\int d^2u\int d^2u'\langle\sqrt{g}v_T^\alpha\omega_\alpha\sqrt{g'}v_T^\beta\omega_\beta\rangle, \tag{4.16}$$

where

$$\mathcal{P}_\perp^{\alpha\beta} = \gamma^\alpha{}_{\alpha'}\gamma^\beta{}_{\beta'}\frac{D^{\alpha'}D^{\beta'}}{\Delta_g}\frac{\delta(\tilde{u}-\tilde{u}')}{\sqrt{g}} = \left(\delta^{\alpha\beta}-\frac{D^\alpha D^\beta}{\Delta_g}\right)\frac{\delta(\tilde{u}-\tilde{u}')}{\sqrt{g}} \tag{4.17}$$

is the transverse projection operator and

$$v_T^\alpha = v^\alpha - A^\alpha \tag{4.18}$$

is manifestly transverse from Eq. (3.18). Thus, as expected, $\Delta\mathcal{F}$ depends only on the transverse part of ω_α.

A longitudinal function such as $\partial_\alpha\phi_e$ maintains its form under coarse graining. A transverse function does not because the direction of a transverse function depends on the local value of the rotation matrix $\gamma^\alpha{}_\beta$. Thus to coarse grain our transverse function $\omega_\alpha(\mathbf{x})$, we set it equal to $\gamma_\alpha{}^\beta\partial_\beta\phi_e$. In the Monge gauge $\partial_\beta\phi_e$ has the same value regardless of the particular configuration of the membrane. Then using $\gamma^\alpha{}_{\alpha'}\gamma^{\alpha'}{}_\beta = -\delta^\alpha_\beta$, we obtain

$$\Delta\mathcal{F} = \frac{1}{2}K\int d^2u\langle\sqrt{g}g^{\alpha\beta}\partial_\alpha\phi_e\partial_\beta\phi_e\rangle - \frac{1}{2}\beta K^2\int d^2u\int d^2u'\langle\sqrt{g}\rho(\mathbf{x})\sqrt{g'}\rho(\mathbf{x}')\rangle \times\phi_e(\mathbf{x})\phi_e(\mathbf{x}'). \tag{4.19}$$

Setting $\epsilon_{\alpha\beta}\partial_\beta\phi_e = \bar{\omega}_\beta^T(\delta_{\alpha\beta}-\partial_\alpha\partial_\beta/\partial^2)$, where $\bar{\omega}_\alpha$ is the coarse-grained ω_α, we find

$$K_R = \frac{1}{A_B}\frac{\partial^2\mathcal{F}}{\partial\bar{\omega}_\alpha^T\partial\bar{\omega}_\alpha^T} = \lim_{q\to0}\left(K\frac{q_\alpha q_\beta}{q^2}\langle\sqrt{g}g^{\alpha\beta}\rangle - \frac{\beta K^2}{q^2}C_{\tilde{\rho}\tilde{\rho}}(\mathbf{q})\right) = K\epsilon_\parallel^{-1}, \tag{4.20}$$

where A_B is the base area and $\epsilon_\parallel = \epsilon_\parallel(q=0)$. Because $\int d^2x\tilde{\rho} = 0$, $C_{\tilde{\rho}\tilde{\rho}}(\mathbf{q})$ tends to zero as $q\to0$ in the ordered phase. We can, therefore, define

$$\begin{aligned}\lim_{q\to0}\frac{1}{q^2}C_{\tilde{\rho}\tilde{\rho}}(\mathbf{q}) &= B\\ &= \lim_{q\to0}\frac{1}{q^2}[C_{\tilde{\rho}\tilde{\rho}}(\mathbf{q})-C_{\tilde{\rho}\tilde{\rho}}(0)]\\ &= \lim_{q\to0}\frac{1}{q^2}\frac{1}{A_B}\int d^2xd^2x'(e^{i\mathbf{q}\cdot(\mathbf{x}-\mathbf{x}')}-1)\\ &\quad\times\langle\tilde{\rho}(\mathbf{x})\tilde{\rho}(\mathbf{x}')\rangle\\ &= -\frac{1}{4}\int d^2x|\mathbf{x}|^2\langle\tilde{\rho}(\mathbf{x})\tilde{\rho}(0)\rangle,\end{aligned} \tag{4.21}$$

where in the final step we used the fact that $\langle\tilde{\rho}(\mathbf{x})\tilde{\rho}(\mathbf{x}')\rangle$ depends only on $\mathbf{x}-\mathbf{x}'$ in translationally invariant systems. Thus

$$K_R = K - \beta K^2 B. \tag{4.22}$$

$C_{\tilde{\rho}\tilde{\rho}}(\mathbf{q})$ is derived in Eq. (4.8).

D. The p-atic correlation function

We have argued that the renormalized rigidity is determined by the dielectric constant associated with ρ rather than that associated with some other combination of the independent charge densities n and S. We will now show that it is indeed this rigidity that controls the long distance properties of the p-atic correlation function $G_p(\mathbf{u},\mathbf{u}')$, [Eqs. (2.31) and (2.38)]. Our calculations follow closely those in Ref. [32] for correlation functions in flat space. To keep things simple, we calculate only to lowest order in height fluctuations in the Monge gauge.

As discussed in Sec. II, the angle θ in Eq. (2.38) can be broken up into a regular part and a singular part: $\theta(\mathbf{x})-\theta(\mathbf{x}') = \theta'(\mathbf{x})-\theta'(\mathbf{x}')+\int_{\mathbf{x}}^{\mathbf{x}'}ds^\alpha v_\alpha$. In addition, we can always choose a gauge so that A_α is purely transverse. In this case θ' decouples from other variables, and we have

$$G_p(\mathbf{x}-\mathbf{x}') = \langle e^{-\frac{1}{2}p^2\langle[\theta'(\mathbf{x})-\theta'(\mathbf{x}')]^2\rangle_g} \times e^{-ip\int_{\mathbf{x}}^{\mathbf{x}'}ds^\alpha(v_\alpha-A_\alpha)}\rangle_{\mathbf{R},v}, \tag{4.23}$$

where $\langle[\theta'(\mathbf{x})-\theta'(\mathbf{x}')]^2\rangle_g$ is evaluated for a fixed metric tensor $g_{\alpha\beta}$ determined by $\mathbf{R}$, and

$$\langle A\rangle_{\mathbf{R},v} = \mathcal{Z}^{-1}\mathrm{Tr}_v y^N\int\mathcal{D}\mathbf{R}e^{-\beta\mathcal{H}_\kappa-\beta\mathcal{H}_{\mathrm{CT}}}A. \tag{4.24}$$

To the order we are working, we can factorize $G_p(\mathbf{x})$ into a "spin-wave" part arising from θ' and a transverse part:

$$G_p(\mathbf{x}) = G_{\mathrm{sw}}(\mathbf{x})G_v(\mathbf{x}), \tag{4.25}$$

where

$$G_{\mathrm{sw}}(\mathbf{x}) = e^{-\frac{1}{2}p^2\langle\langle[\theta'(\mathbf{x})-\theta'(\mathbf{x}')]^2\rangle_g\rangle} \tag{4.26}$$

and

$$G_v(\mathbf{x}) = e^{-\frac{1}{2}p^2\langle(\Delta\theta_v)^2\rangle} = e^{-\frac{1}{2}p^2g_v(\mathbf{x})}, \tag{4.27}$$

where $\Delta\theta_v = \int_{\mathbf{x}}^{\mathbf{x}'}ds^\alpha(v_\alpha-A_\alpha)$ and the double brackets in Eq. (4.26) refers to an average over θ followed by an average over $\mathbf{R}$. In the Monge gauge, to the order we are working,

$$\langle[\theta'(\mathbf{x})-\theta'(\mathbf{x}')]^2\rangle_g = \frac{2}{\beta K}\mathcal{G}(\mathbf{x}-\mathbf{x}'), \tag{4.28}$$

where

$$\mathcal{G}(\mathbf{x}-\mathbf{x}') = \left(\frac{1}{\nabla^2}\right)_{\mathbf{x}\mathbf{x}'} = \frac{1}{2\pi}\ln\frac{|\mathbf{x}-\mathbf{x}'|}{a}. \tag{4.29}$$

Thus

$$G_{\mathrm{sw}}(\mathbf{x}) = |\mathbf{x}|^{-p^2/2\pi\beta K}. \tag{4.30}$$

To evaluate $G_v(\mathbf{x})$, we use Eq. (3.18) to lowest order in the Monge gauge to obtain

$$\Delta\theta_v = \epsilon_{\alpha\beta}\int_{\mathbf{x}}^{\mathbf{x}'}d^2y\rho(y)f(y), \tag{4.31}$$

where

$$f(y) = \int_{\mathbf{x}}^{\mathbf{x}'} ds^{\alpha} \epsilon_{\alpha\beta} \partial_{\beta}^{s} \mathcal{G}(\mathbf{s}-\mathbf{y}). \tag{4.32}$$

Then using the Cauchy-Riemman relation,

$$\begin{aligned} \epsilon_{\alpha\beta}\partial_{\beta}\mathcal{G}(\mathbf{x}) &= -\partial_{\alpha}\mathcal{G}_{\perp}(\mathbf{x}) \ , \\ \epsilon_{\alpha\beta}\partial_{\beta}\mathcal{G}_{\perp}(\mathbf{x}) &= \partial_{\alpha}\mathcal{G}(\mathbf{x}), \end{aligned} \tag{4.33}$$

where $\mathcal{G}_{\perp}(\mathbf{x}) = (1/2\pi)\tan(y/x)$, we find

$$f(y) = -[\mathcal{G}_{\perp}(\mathbf{x}'-\mathbf{y}) - \mathcal{G}_{\perp}(\mathbf{x}-\mathbf{y})] \tag{4.34}$$

and

$$\begin{aligned} G_{\mathrm{v}}(\mathbf{x}-\mathbf{x}') &= \int d^2y d^2y' \langle \rho(\mathbf{y})\rho(\mathbf{y}')\rangle f(\mathbf{y}) f(\mathbf{y}') \\ &= -\frac{1}{2}\int d^2y d^2y' \langle \rho(\mathbf{y})\rho(\mathbf{y}')\rangle [f(\mathbf{y}) - f(\mathbf{y}')]^2. \end{aligned} \tag{4.35}$$

Setting $\mathbf{y} = \mathbf{R} + \mathbf{r}/2$ and $\mathbf{y}' = \mathbf{R} - \mathbf{r}/2$, and expanding in $\mathbf{r}$, we obtain

$$\begin{aligned} G_v(\mathbf{x}-\mathbf{x}') = -\frac{1}{2}\int d^2r \langle \rho(\mathbf{r})\rho(0)\rangle r_{\alpha} r_{\beta} \\ \times \int d^2R \partial_{\alpha} f(\mathbf{R}) \partial_{\beta} f(\mathbf{R}). \end{aligned} \tag{4.36}$$

Then using Eqs. (4.21), (4.34), (4.36), and $\nabla_R^2 \mathcal{G}(\mathbf{s}-\mathbf{R}) = \delta(\mathbf{s}-\mathbf{R})$, we find

$$\begin{aligned} G_{\mathrm{v}}(\mathbf{x}-\mathbf{x}') &= 2B[\mathcal{G}(\mathbf{x}-\mathbf{x}') - \mathcal{G}(0)] \\ &\sim \frac{2B}{2\pi} \ln \frac{|\mathbf{x}-\mathbf{x}'|}{a}, \end{aligned} \tag{4.37}$$

where we have treated $\mathcal{G}(0)$ as a nondivergent constant because $(\mathbf{x}-\mathbf{x}')$ is restricted to be greater than a.

Combining Eqs. (4.25), (4.27), (4.30), and (4.37), we obtain

$$\begin{aligned} G_p &= |\mathbf{x}|^{-p^2/2\pi\beta K} |\mathbf{x}|^{-p^2 B/2\pi} \\ &= |\mathbf{x}|^{-p^2/2\pi\beta K_R} \end{aligned} \tag{4.38}$$

with

$$(\beta K_R)^{-1} = (\beta K)^{-1} + B. \tag{4.39}$$

This equation agrees with Eq. (4.22) to lowest order in B.

E. Evaluation of the dielectric constant

As we discussed at the beginning of this section, the correlation function $C_{\tilde{\rho}\tilde{\rho}}(\mathbf{q})$ must be evaluated in the presence of all interactions including that arising from the Liouville term. In this subsection, we will derive a general expression for $C_{\tilde{\rho}\tilde{\rho}}(\mathbf{q})$, which we will evaluate in the low-temperature, low-fugacity limit. We will also discuss effective Coulomb interactions. Both κ and K have units of energy. Thus, both $(\beta\kappa)^{-1}$ and $(\beta K)^{-1}$ are unitless measures of temperature. In addition, either of these quantities multiplied by any function of the ratio K/κ is also a measure of temperature. In our low-temperature expansion, we will require $A\beta K/(\beta\kappa)^2 = A(T/\kappa)(K/\kappa)$, where A smaller than $1/(2\pi)$, as well as $(\beta\kappa)^{-1}$ and $(\beta K)^{-1}$ to be small. Thus, we will not consider the limit $K \to \infty$. We will. nonetheless, be able to explore a large region of the phase diagram.

The evaluation of $C_{\tilde{\rho}\tilde{\rho}}(\mathbf{q})$ is obtained most directly in terms of diagrams. Figure 3 shows the basic ingredients of a diagrammatic perturbation theory: the height propagator $G_{hh}(\mathbf{q}) = (\beta\kappa q^4)^{-1}$, the three Coulomb interactions [Eq. (3.24)] K'/q^2, K/q^2, and K/q^2 coupling, respectively, $\tilde{S}$ to $\tilde{S}$, $\tilde{n}$ to $\tilde{n}$ and $\tilde{S}$ to $\tilde{n}$, the $\tilde{n}-\tilde{n}$ propagator when $\mathcal{H}_{nS}$ is zero, and nonlinear vertices arising from the curvature. The total Coulomb Hamiltonian of Eq. (3.24) contains $S-S$ and $n-n$ terms and a part

$$\mathcal{H}_{nS} = -K \int d^2u \sqrt{g} n \left(-\frac{1}{\Delta_g}\right) \sqrt{g} S \tag{4.40}$$

coupling n to S. We will first calculate correlation functions when $\mathcal{H}_{nS}$ is zero. Then we will calculate the effects of turning on $\mathcal{H}_{nS}$. If $\mathcal{H}_{nS}$ is zero, then $C_{\tilde{n}\tilde{S}}$ where $\tilde{S} = \sqrt{g}S$ is zero, and the Gaussian curvature correlation function $C_{\tilde{S}\tilde{S}}$ is simply that of a Coulomb gas with coupling K'. It can be represented as a sum of polarization bubbles shown in Fig. 4 linked by a Coulomb interaction as shown in Fig. 5. The result is

$$C^0_{\tilde{S}\tilde{S}}(\mathbf{q}) = \frac{\mathcal{P}(\mathbf{q})}{1 + (K'/q^2)\mathcal{P}(\mathbf{q})}. \tag{4.41}$$

To lowest order in h, the Gaussian curvature is

$$S = \frac{1}{2}(\nabla^2 h \nabla^2 h - \partial_i\partial_j h \partial_i\partial_j h), \tag{4.42}$$

and, to lowest order in $(\beta\kappa)^{-1}$, $\mathcal{P}(\mathbf{q})$ is determined by diagram (a) in Fig. 4:

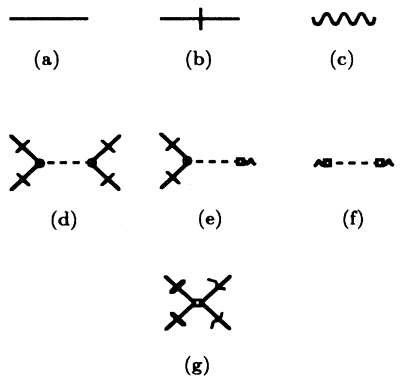

FIG. 3. Elements for constructing a diagrammatic perturbation expansion for a Coulomb gas on a fluctuating membrane: (a) The height propagator $G_{hh} = 1/(\beta\kappa q^4)$, (b) the height propagator with two gradients represented by the vertical lines, (c) the bare vortex charge-density propagator $C^0_{\tilde{n}\tilde{n}}$ [Eq. (4.44)], (d) the Coulomb vertex K'/q^2 in $\mathcal{H}_{SS}$, (e) the Coulomb vertex $-K/q^2$ in $\mathcal{H}_{nS}$, (f) the Coulomb vertex K/q^2 in $\mathcal{H}_{nn}$, and (g) a nonlinear vertex from the curvature energy [Eq. (3.2)].

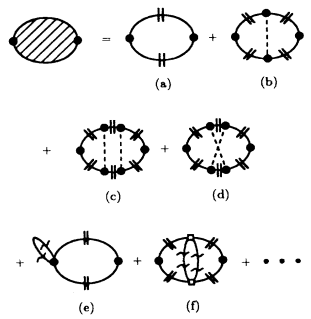

FIG. 4. Diagrammatic contributions to the polarization bubble $\mathcal{P}$ represented by the cross-hatched diagram to the left of the equal sign. The components of these diagrams are defined in Fig. 3. The leading-order contribution to $\mathcal{P}$ is given by diagram (a). Diagram (e) is the first correction to $\mathcal{P}$ arising from the $\sqrt{g}$ factors in the definition of $\mathcal{P}$. The double cross lines on the height propagators represent the gradients, with appropriate symmetry, in the Gaussian curvature [Eq. (4.42)].

$$\mathcal{P}(\mathbf{q}) = \frac{1}{2}\frac{1}{(\beta\kappa)^2}\int \frac{d^2k}{(2\pi)^2}\frac{(\mathbf{q}\times\mathbf{k})^4}{k^4(\mathbf{k}+\mathbf{q})^4} = \frac{3}{32\pi}\frac{q^2}{(\beta\kappa)^{-2}}. \tag{4.43}$$

Note that $\mathcal{P}(\mathbf{q})$ is proportional to q^2 even though the numerator in the integrand is proportional to q^4. There is an infrared singularity in the integral over $\mathbf{k}$ that converts the q^4 to the q^2. Higher-order contributions to $\mathcal{P}$ are shown in Figs. 4(b)–4(f). The contribution to $\mathcal{P}$ from Fig. 4(b) is of order $q^2\beta K/(\beta\kappa)^4$, i.e., of order $\beta K/(\beta\kappa)^2$ smaller than Eq. (4.43). The diagrams of Figs. 4(c) and 4(d) are smaller by another factor of $\beta K/(\beta\kappa)^2$. The diagram in Fig. 4(e), which arises from the $\sqrt{g}$ factor and nonlinear terms in $\tilde{S}$, is of order $(\beta\kappa)^{-1}$ times Eq. (4.43). It, however, has an infrared divergence, which would have to be handled with care if we wished to calculate to the next order in T. The diagram in Fig. 4(f) is of order $(\beta\kappa)^{-4}$.

When $\mathcal{H}_{nS} = 0$, the disclination correlation function $C_{\tilde{n}\tilde{n}}(\mathbf{q})$ can be calculated as a power series in y. To lowest order in T, we can replace $\sqrt{g}$ by 1 in $\tilde{n}$. Then to lowest order in y,

$$C^0_{\tilde{n}\tilde{n}}(\mathbf{q}) = \frac{1}{A_B}\frac{1}{\mathcal{Z}}y^2\int\mathcal{D}\mathbf{R}\int\frac{d^2x_+}{a^2}\frac{d^2x_-}{a^2}\langle n(\mathbf{q})n(-\mathbf{q})\rangle \times e^{-\beta\mathcal{H}_\kappa-\beta\mathcal{H}_{SS}-\beta\mathcal{H}_{nn}}, \tag{4.44}$$

where $n(\mathbf{q}) = (2\pi/p)(e^{i\mathbf{q}\cdot\mathbf{x}_+} - e^{-i\mathbf{q}\cdot\mathbf{x}_-})$. Therefore

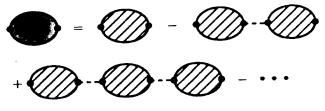

FIG. 5. Diagrammatic representation of the full $C^0_{\tilde{n}\tilde{n}}$ propagator when $\mathcal{H}_{nS} = 0$.

FIG. 6. A representative additional diagram contributing to $\mathcal{P}$ when $\mathcal{H}_{nS}$ is turned on. The expansion for $C^0_{\tilde{n}\tilde{n}}$ is still given by Eq. (4.44) and Fig. 5.

$$C^0_{\tilde{n}\tilde{n}}(\mathbf{q}) = y^2\left(\frac{2\pi}{p}\right)^2\frac{1}{2}q^2\int_a^\infty d^2x|\mathbf{x}|^{2-2\pi\beta K} = \frac{4\pi^3}{p^2}y^2q^2\int_a^\infty drr^{3-2\pi\beta K} + O(y^4). \tag{4.45}$$

When $\mathcal{H}_{nS}$ is turned on, there will be additional contributions to the polarization bubble such as shown in Fig. 6. The correlation functions $C_{\tilde{n}\tilde{n}}$, $C_{\tilde{S}\tilde{S}}$, and $C_{\tilde{n}\tilde{S}}$ can be obtained from the diagrams in Fig. 7:

$$C_{\tilde{n}\tilde{n}} = \frac{C^0_{\tilde{n}\tilde{n}}}{1-(\beta^2K^2/q^4)C^0_{\tilde{n}\tilde{n}}C^0_{\tilde{S}\tilde{S}}}, \tag{4.46}$$

$$C_{\tilde{S}\tilde{S}} = \frac{C^0_{\tilde{S}\tilde{S}}}{1-(\beta^2K^2/q^4)C^0_{\tilde{n}\tilde{n}}C^0_{\tilde{S}\tilde{S}}} = \frac{\mathcal{P}}{1+(\beta K'/q^2)\mathcal{P}-\beta^2K^2\mathcal{P}C^0_{\tilde{n}\tilde{n}}}, \tag{4.47}$$

$$C_{\tilde{n}\tilde{S}} = \frac{\beta K}{q^2}\frac{C^0_{\tilde{n}\tilde{n}}C^0_{\tilde{S}\tilde{S}}}{1-(\beta^2K^2/q^4)C^0_{\tilde{n}\tilde{n}}C^0_{\tilde{S}\tilde{S}}}, \tag{4.48}$$

where $C^0_{\tilde{S}\tilde{S}}$ is given by Eq. (4.43) with $\mathcal{P}(\mathbf{q})$ corrected by a contribution such as that in Fig. 6. Combining Eqs. (4.47) and (4.48), we obtain the charge-density correlation function determining K_R:

$$\begin{aligned} C_{\tilde{\rho}\tilde{\rho}}(\mathbf{q}) &= C_{\tilde{n}\tilde{n}}(\mathbf{q}) - 2C_{\tilde{n}\tilde{S}}(\mathbf{q}) + C_{\tilde{S}\tilde{S}}(\mathbf{q}) \\ &= \frac{C^0_{\tilde{n}\tilde{n}}(\mathbf{q}) - 2(\beta K/q^2)C^0_{\tilde{n}\tilde{n}}(\mathbf{q})C_{\tilde{S}\tilde{S}}(\mathbf{q}) + C_{\tilde{S}\tilde{S}}(\mathbf{q})}{1-(\beta^2K^2/q^4)C^0_{\tilde{n}\tilde{n}}(\mathbf{q})C_{\tilde{S}\tilde{S}}(\mathbf{q})} \\ &= \frac{\mathcal{P}(\mathbf{q}) + C^0_{\tilde{n}\tilde{n}}(\mathbf{q})[1-(\beta(2K-K')/q^2)\mathcal{P}(\mathbf{q})]}{1+(\beta K/q^2)\mathcal{P}(\mathbf{q})[(K'/K)-(\beta\kappa/q^2)C^0_{\tilde{n}\tilde{n}}(\mathbf{q})]}. \end{aligned} \tag{4.49}$$

In the limit of low temperature and low fugacity, this

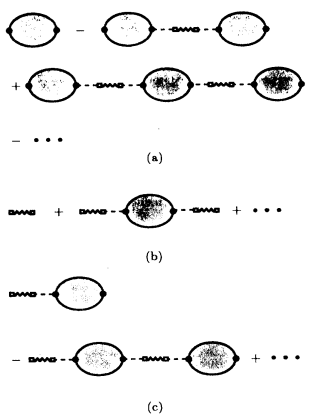

FIG. 7. Diagrammatic expansion of (a) $C_{\tilde{n}\tilde{n}}$, (b) $C_{\tilde{S}\tilde{S}}$, and (c) $C_{\tilde{n}\tilde{S}}$. The bubble is $C^0_{\tilde{n}\tilde{n}}$ represented in Fig. 5.

reduces to

$$C_{\hat{\rho}\hat{\rho}}(\mathbf{q}) \simeq \mathcal{P}(\mathbf{q}) + C^0_{\hat{n}\hat{n}}(\mathbf{q})\left(1 - 2\frac{\beta K}{q^2}\mathcal{P}(\mathbf{q})\right) + \cdots, \tag{4.50}$$

where $\mathcal{P}(\mathbf{q})$ is given by Eq. (4.43) and $C^0_{\hat{n}\hat{n}}(\mathbf{q})$ by Eq. (4.45). The second term in the coefficient of $C^0_{\hat{n}\hat{n}}$ is of order $\beta K/(\beta\kappa)^2$ and will be neglected.

We can now calculate the dielectric constant or renormalized rigidity to lowest order in temperature and fugacity using Eqs. (4.21), (4.22), (4.43), (4.45) and (4.50).

$$\beta K_R = \beta\overline{K} - (\beta\overline{K})^2\frac{4\pi^3}{p^2}y^2\int_a^\infty dr r^{3-2\pi\beta\overline{K}}, \tag{4.51}$$

where

$$\beta\overline{K} = \beta K - \frac{3}{32\pi}\left(\frac{K}{\kappa}\right)^2. \tag{4.52}$$

we assume $(3/32\pi)\beta K/(\beta\kappa)^2 \ll 1$ so that

$$(\beta\overline{K})^{-1} = (\beta K)^{-1} + \frac{3}{32\pi}(\beta\kappa)^{-2}. \tag{4.53}$$

Thus, the equation for βK_R is identical to that for a rigid flat membrane but with $\overline{K}$ replacing K.

V. RENORMALIZATION EQUATIONS

To determine the properties of the Kosterlitz-Thouless transition on a fluctuating membrane, we need to determine the renormalization flow equations for κ, K, and y. Equation (4.51) for K_R is identical to the equation for K_R on a flat membrane [4] with K replaced by $\overline{K}$. Flow equations for $\overline{K}(l)$ and $y(l)$ can be obtained in the usual way [32] from Eq. (4.51). By breaking up the integral $\int_a^\infty dr$ into $\int_a^{ae^l} dr + \int_{ae^l}^\infty dr$, putting the first part into a renormalized $\overline{K}(l)$, and rescaling the second part by $r \to re^{-l}$, we obtain

$$(\beta K_R)^{-1} = [\beta\overline{K}(l)]^{-1} + \frac{4\pi^3}{p^2}y^2(l)\int_a^\infty dr r^{3-2\pi\beta K} \tag{5.1}$$

with

$$\frac{d(\beta\overline{K})^{-1}}{dl} = \frac{4\pi^3}{p^2}y^2, \tag{5.2}$$

$$\frac{dy}{dl} = \left(2 - \frac{\pi\beta\overline{K}}{p^2}\right)y. \tag{5.3}$$

Observe that the bending rigidity does not appear explicitly in these equations; it only appears via the dependence of $\beta\overline{K}$ on κ. This suggests that there should be an effective theory for a flat membrane with a bare hexatic rigidity equal to $\overline{K} = K - (3/32\pi)(K/\kappa)^2$ rather than K. Indeed, if we integrate our height fluctuations to produce an effective flat-space Hamiltonian via

$$e^{-\beta\mathcal{H}_{\rm eff}} = \int \mathcal{D}h e^{-\beta\mathcal{H}_\kappa - \beta\mathcal{H}_\theta}, \tag{5.4}$$

we obtain

$$\mathcal{H}_{\rm eff} = \tfrac{1}{2}\beta\overline{K}\int d^2x(\nabla\theta)^2. \tag{5.5}$$

Thus, the fluctuating membrane behaves like a flat membrane with a hexatic rigidity $\overline{K}$. Note that the renormalized rigidity $\overline{K}$ appears in Eq. (5.5) because fluctuations at *all* wave numbers $\mathbf{q}$ have been integrated out. If we had calculated an effective Hamiltonian by removing $h(\mathbf{q})$ for $\mathbf{q}$ within a shell $\Lambda/b < q < \Lambda$, there would have been no shift in K.

The renormalization of κ can be calculated using Eqs. (3.23) and (3.24). Diagrams contributing to the renormalized bending rigidity κ_R to lowest order in β^{-1} are shown in Fig. 8. They yield

$$\begin{aligned}\beta\kappa_R &= \beta\kappa - \frac{3}{4\pi}\int_{L^{-1}}^\Lambda\frac{dq}{q} + \frac{3}{4\pi}\frac{\beta K'}{4\beta\kappa}\int_{L^{-1}}^\Lambda\frac{dq}{q} + \frac{3}{4\pi}\frac{\pi^3y^2}{p^2}\frac{(\beta K')^2}{4\beta\kappa}\left(\int_{L^{-1}}^\Lambda\frac{dq}{q}\right)^2 \\ &= \beta\kappa - \frac{3}{4\pi}\left(1 - \frac{\beta K'}{4\beta\kappa}\right)\int_a^L\frac{dr}{r} + \frac{3}{4\pi}\frac{\pi^3y^2}{p^2}\frac{(\beta K')^2}{4\beta\kappa}\left(\int_a^L\frac{dr}{r}\right)^2,\end{aligned} \tag{5.6}$$

where L is the linear dimension of the membrane, which we take to be infinite, and $\Lambda = 1/a$. We can now follow exactly the same procedure to obtain the recursion relation for κ we used to obtain those for $\overline{K}$ and y. To lowest order in $(\beta\kappa)^{-1}$, we can replace K' by K. We break the integral $\int_a^\infty$ into two parts, and rescale to obtain

$$\frac{d\beta\kappa}{dl} = -\frac{3}{4\pi}\left(1 - \frac{\beta K}{4\beta\kappa}\right). \tag{5.7}$$

This equation was derived from the low-order diagrams shown in Fig. 8 in which the Coulomb energy K/q^2 is treated as a perturbation. One can also structure a perturbation theory in which the Coulomb propagator K'/q^2

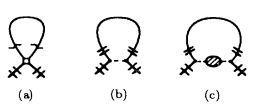

FIG. 8. Diagrams for the bending rigidity κ.

coupling $\tilde{S}$ to $\tilde{S}$ [Eq. (3.24)] is replaced by $K'/\epsilon_{\parallel,\tilde{S}\tilde{S}}q^2$ where

$$\epsilon^{-1}_{\parallel,\tilde{S}\tilde{S}}(\mathbf{q}) = 1 - \frac{K'}{q^2}C_{\tilde{S}\tilde{S}}(\mathbf{q}) - \frac{K}{K'}\frac{1}{q^2}C_{\tilde{n}\tilde{n}} + \frac{2K}{q^2}C_{\tilde{n}\tilde{S}} \quad (5.8)$$

as shown in Fig. 9. Similar expressions can be derived for the effective Coulomb potentials coupling $\tilde{n}$ to $\tilde{n}$ and $\tilde{n}$ to $\tilde{S}$. In this scheme, Figs. 8(b) and 8(c) are replaced by Fig. 9(a). In addition, there are higher-order diagrams such as those shown in Fig. 9(b). These diagrams have two or more loops and are difficult to treat using our naive renormalization scheme. In the companion paper [15], we employ a controlled regularization scheme to treat these graphs using the sine-Gordon Hamiltonian. It shows that K should be replaced by $\overline{K}$ in Eq. (5.7). Thus we have

$$\frac{d\beta\kappa}{dl} = -\frac{3}{4\pi}\left(1 - \frac{\beta\overline{K}}{4\beta\kappa}\right). \quad (5.9)$$

The renormalization flow equations now depend on $\overline{K}$ and not on K. They also do not contain a term proportional to y^2. The derivation of the latter result will be discussed in more detail in the companion paper on the sine-Gordon theory.

Equations (5.2), (5.3), and (5.9) define renormalization flows for fluctuating hexatic membranes. They have a fixed point at

$$\beta\overline{K}^* = \frac{2p^2}{\pi}, \qquad y^* = 0, \qquad \beta\kappa^* = \beta\frac{\overline{K}^*}{4} = \frac{p^2}{2\pi}. \quad (5.10)$$

We can obtain equations in the vicinity of this fixed point by defining

$$\beta\overline{K} = \beta\overline{K}^*(1-x), \qquad \beta\kappa = \beta\kappa^*(1-z). \quad (5.11)$$

Then

$$\frac{dx}{dl} = 8\pi^2 y^2, \qquad \frac{dy}{dl} = 2xy\ , \quad (5.12)$$

$$\frac{dz}{dl} = \frac{3}{2p^2}\frac{x-z}{1-z}. \quad (5.13)$$

The flow lines for these equations are shown in Figs. 10 and Fig. 11. Figure 10(a) shows flows in the xy plane, which are identical to those in flat space [4]. Figure 10(b) shows flows in the yz plane, which are similar to those in the xy plane. Figure 11(a) shows flows in the $(\beta\overline{K})^{-1}$-$(\beta\kappa)^{-1}$ plane. As in previous treatments [8], there is a fixed line in this plane at $\beta\kappa = \beta\overline{K}/4$ ($x = z$), and the crinkled-to-crumpled transition occurs at $\beta\overline{K} = \beta\overline{K}^*$ independent of $\beta\kappa$, and the Kosterlitz-Thouless transition

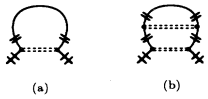

FIG. 9. Diagrams contributing to κ in terms of the screened Coulomb propagator (represented by the double-dashed line) $K'/(\epsilon_{\parallel,ss}q^2)$ defined in Eq. (5.8).

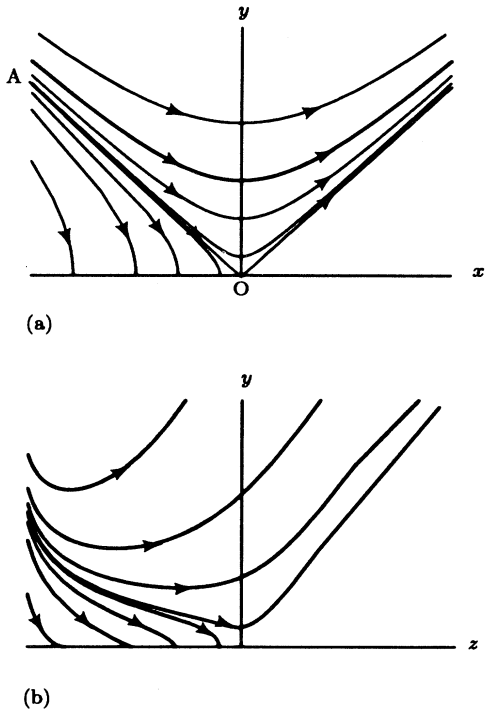

FIG. 10. (a) Renormalization flows in the xy plane. These are identical to the order of our calculations to those of the flat space xy model. The separatrix AO is the critical line. (b) Flows in the zy plane. They are similar to those in the xy plane.

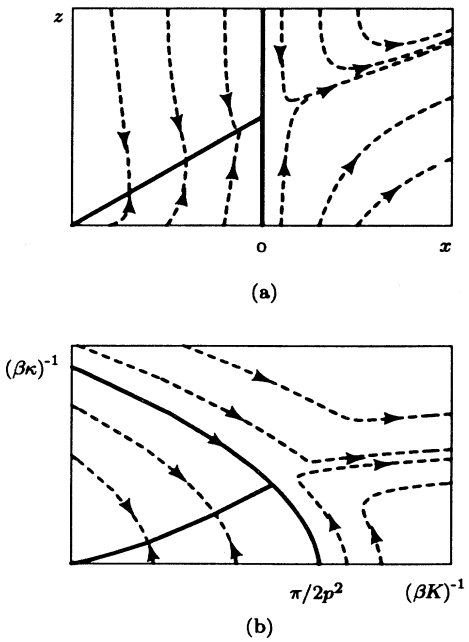

FIG. 11. (a) Renormalization flows in the xz plane. The transition from the crinkled to the crumpled phase takes place at $x = 0$ independent of z (i.e., independent of $\beta\kappa$), in agreement with previous calculations [9]. (b) Flows in the $(\beta K)^{-1}$-$(\beta\kappa)^{-1}$ plane. Here, there is a transition from the crinkled to the crumpled phase as κ is decreased.

occurs at $x = 0$ independent of z.

The separatrix AO in Fig. 10(a) is the transition line dividing the crinkled hexatic phase from the melted crumpled phase. Systems whose initial values of x and y lie below and to the left of the separatrix flow to the low-temperature crinkled hexatic phase; points above and to the right of the separatrix flow away to the crumpled fluid. The initial value of x is $x_0 = 1 - \overline{K}/\overline{K}^*$, which increases with decreasing $\beta\overline{K} = \beta K - (3/32\pi)(K/\kappa)^2$. Decreasing the bending rigidity κ decreases $\overline{K}$ and eventually drives x to the right of the separatrix. Thus, there will be a transition from the crinkled to the crumpled phase as κ is decreased. An alternative way to see this is to use K rather than $\overline{K}$ as the independent variable. To do this, we define $K(l)$ to satisfy Eq. (4.52) with $\overline{K}$ and κ replaced, respectively, by $\overline{K}(l)$ and $\kappa(l)$. Flows in the $([\beta K(l)]^{-1}, [\beta\kappa(l)]^{-1})$ plane are shown in Fig. 11(b). The vertical transition line in the $([\beta\overline{K}(l)]^{-1}, [\beta\kappa(l)]^{-1})$ plane is now curved and crosses the $(\beta K)^{-1} = 0$ axis at a finite value of $(\beta\kappa)^{-1}$. Points to the left and below the separatrix flow to the crinkled fixed line. Points outside it flow to the crumpled phase.

In deriving our recursion relations, we restricted ourselves to $(\beta\kappa)^{-1}$, $(\beta K)^{-1}$, and $\beta K/(\beta\kappa)^2 < 2\pi$. Thus, our calculations, strictly speaking, only apply below the curves OA in Figs. 2 and 11(b). The flows in Fig. 11 we calculated for $p = 1$. Figure 2 shows flows for the physically more interesting case of $p = 6$. Our approximation applies to a considerable region around the fixed point P. Higher-order terms in $(\beta\kappa)^{-1}$ and $\beta K/(\beta\kappa)^2$ would have to be included to get an accurate picture of what happens above the curve OA. Is seems likely to us, however, that these higher-order terms will not lead to any qualitative modifications to Fig. 2. For any finite value of K^{-1} and κ^{-1}, the crinkled-to-crumpled transition is governed by the fixed point P. For infinite hexatic rigidity, $K^{-1} = 0$, the transition is controlled by different physics, probably analogous to that of tethered membranes [10]. There could, of course, be some phase boundary at large $\beta K/(\beta\kappa)^2$ separating $K = \infty$-like behavior from finite-K behavior, but we do not see any particular reason why this should be so.

The persistence length in the fluid phase is

$$\xi_p = ae^{l^*}, \tag{5.14}$$

where l^* is determined by

$$\beta\kappa(l^*) = \beta\kappa^*[1 - z(l^*)] = 0, \tag{5.15}$$

i.e., by $z(l^*) = 1$. Integration of Eqs. (5.12) and (5.13) yield $z(l)$ and thus ξ_p. Equation (5.13) for z is a nonlinear and cannot be determined analytically. We can, however, obtain a very good estimate of ξ_p when $\xi_p > \xi_{\rm KT}$, where $\xi_{\rm KT} \sim a\exp(b/|T - T_{\rm KT}|^{1/2})$ is the Kosterlitz-Thouless correlation length. The latter length is $\xi_{\rm KT} = ae^{l_0}$, where $\beta\overline{K}(l_0) = 0$ or $x(l_0) = 1$. The recursion relation, Eq. (5.9) for $z(l)$ is only valid for $\overline{K} > 0$. When $\overline{K} \to 0$, we approach a fluid phase with recursion relations for κ determined by κ alone. We, therefore, assume that $x(l) = 0$ for $l > l_0$. Then

$$\frac{dz}{dl} = \frac{3}{2p^2}, \qquad l > l_0. \tag{5.16}$$

This equation can be integrated subject to the boundary condition that $z(l_0)$ be the value of $z(l)$ at $l = l_0$ determined by Eqs. (5.2) and (5.11). Thus,

$$z(l) = z(l_0) + \frac{3}{2p^2}(l - l_0), \tag{5.17}$$

$l^* = l_0 + 2p^2[1 - z(l_0)]/3$, and

$$\xi_p = ae^{l^*} = \xi_{\rm KT}e^{4\pi\beta\kappa(l_0)/3}, \tag{5.18}$$

where we used $\beta\kappa(l_0) = p^2[1 - z(l_0)]/(2\pi)$. This expression is to be compared with the result $\xi_p = ae^{4\pi\beta\kappa/3}$ for a pure fluid membrane. It is what one would naively have expected. The microscopic length a is replaced by the KT coherence length $\xi_{\rm KT}$, and κ at length scale a is replaced by κ at a length scale $\xi_{\rm KT}$. Equation (5.18) for ξ_p is valid provided $\xi_p > \xi_{\rm KT}$ (or $l^* > l_0$). Near the KT critical point, this inequality may not be satisfied.

VI. REVIEW AND DISCUSSION

We have investigated the Kosterlitz-Thouless transition on fluctuating hexatic membranes. We developed three equivalent Hamiltonians for describing these membranes: the hexatic elastic Hamiltonian expressed in terms of gradients of the hexatic angle variable, a Coulomb-gas Hamiltonian, and a sine-Gordon Hamiltonian. The Coulomb gas is characterized by Gaussian curvature and disclination charge densities, which interact via potentials partially determined by the Liouville action arising from a covariant cutoff. The sine-Gordon Hamiltonian has a linear coupling between the sine-Gordon field and Gaussian curvature. We showed that height fluctuations, when integrated over all wave number, soften the hexatic stiffness K. As a result, the disclination melting transition from the hexatic crinkled phase to the fluid crumpled phase is brought about both by increasing temperature and by decreasing the bending rigidity κ. We derived renormalization-group recursion relations for K, κ, and the disclination fugacity y that explicitly verify this. In a Ref. [15], we provide an alternative derivation of these recursion relations using the sine-Gordon Hamiltonian.

Though the picture we present of the Kosterlitz-Thouless transition from the hexatic crinkled phase to the crumpled fluid phase makes a great deal of sense, it does leave some incompletely answered or unanswered questions. First, we believe that the nature of shape fluctuation in the crinkled phase is not completely resolved. It is generally believed [8] that the crinkled phase is characterized by power-law correlations in layer normals: $\langle \mathbf{N}(\mathbf{x}) \cdot \mathbf{N}(0)\rangle \sim |\mathbf{x}|^{-\eta}$, where $\eta = 2T/(\pi K)$. This result is obtained via exponentiation of the expansion

$$\begin{aligned}\langle \mathbf{N}(\mathbf{x}) \cdot \mathbf{N}(0)\rangle &\approx 1 - \tfrac{1}{2}\langle[\nabla h(\mathbf{x}) - \nabla h(0)]^2\rangle \\ &= 1 - \frac{T}{2\pi\kappa}\ln(|\mathbf{x}|/a)\ ,\end{aligned} \tag{6.1}$$

using $\kappa = K/4$. The exponentiation of this series has not been explicitly justified with, for example, a calculation of second-order terms in $(T/\kappa)\ln(\mathbf{x}/a)$. It is interesting to note that the de Gennes–Taupin persistence length [33] $\xi_{\rm GT} = ae^{2\pi\kappa/T}$ beyond which a fluid membrane is crumpled was calculated using Eq. (6.1) and setting $\langle \mathbf{N}(\mathbf{x}) \cdot \mathbf{N}(0) \rangle = 0$. This observation would suggest that the possibility that the crinkled phase is in fact crumpled, but with a longer persistence length than the fluid phase, cannot be ruled out.

Second, we have in our calculations imposed a constraint of charge neutrality. In flat membranes (i.e., films), this constraint is imposed by the prohibitive energy cost of having excess charge of either sign. We believe that there is a similar energy cost for breaking charge neutrality in free membranes, which are not constrained to be flat, though the situation here is more complicated. Nelson [14] has pointed out that the plus-minus symmetry present in flat membranes is broken in free membranes. Membranes with a single disclination undergo a mechanical buckling transition from a flat configuration to a cone configuration for a positive disclination or a saddle configuration for a negative disclination [34]. The energy of the cone is lower than that of the saddle, though both energies are proportional to $\ln(R/a)$, where R is the linear dimension of the membrane. Does this asymmetry modify the picture presented in this paper? We believe not. A free membrane will choose configurations that will minimize its free energy. Any configuration, whether flat or buckled, with an excess of one sign of charge will have a contribution to its energy proportional to $\ln(R/a)$. Charge neutral configurations, on the other hand, have energies that are finite in the $R \to \infty$ limit. Thus, there is a prohibitive energy cost in both flat and free membranes to the violation of charge neutrality. The shape of a membrane near the core of positive and negative disclination may nonetheless differ and lead to different fugacities y_+ and y_-. We generalize our treatment to include this possibility in Ref. [15]. The results are that the ratio of the two fugacities is a marginal variable. In the ordered phase, both y_+ and y_- scale to zero, and the KT transition to the disordered phase is not affected. In the disordered phase, both fugacities grow with a fixed ratio. A more complete treatment of Gaussian curvature will be needed to interpret this result.

ACKNOWLEDGMENTS

We are grateful to Mark Bowich, David Nelson, Phil Nelson, Burt Ovrut, and Leo Radzihovski for helpful conversations. This work was supported in part by the Penn Laboratory for Research in the Structure of Matter under NSF Grant No. 91-20668. Further support was provided by the Institute for Theoretical Physics (under NSF Grant No. 89-04035), where a portion of this work was carried out.

[1] D.R. Nelson, T. Piran, and S. Weinberg, in *Proceedings of the V Jerusalem Winter School* (World Scientific, Singapore, 1989).
[2] *The Structure and Conformation of Amphiphilic Membranes*, eidted by R. Lipowsky, D. Richter, and K. Kremer (Springer, Berlin, 1992).
[3] D.R. Nelson and B.I. Halperin, Phys. Rev. B **19**, 2457 (1979).
[4] J.M. Kosterlitz and D.J. Thouless, J. Phys. C **5**, 1124 (1972); **6**, 1181 (1973).
[5] D.R. Nelson, in *Phase Transitions and Critical Phenomena*, edited by C. Domb and J. Lebowitz (Academic, New York, 1983), Vol. 7.
[6] P. Minnhagen, Rev. Mod. Phys. **59**, 1001 (1987).
[7] D.R. Nelson and L. Peliti, J. Phys. (Paris) **48**, 1085 (1987).
[8] F. David, E. Guitter, and L. Peliti, J. Phys. (Paris) **48**, 2059 (1987).
[9] E. Guitter and M. Kardar, Europhys. Lett. **13**, 441 (1990).
[10] Y. Kantor, M. Kardar, and D.R. Nelson, Phys. Rev. Lett. **57**, 791 (1986): Phys. Rev. A **35**, 3056 (1987); M. Paczuski, M. Kardar, and D.R. Nelson, Phys. Rev. Lett. **60**, 2638 (1988); J. A. Aronovitz, L. Golubović, and T.C. Lubensky, J. Phys. (Paris) **50**, 609 (1988).
[11] H.S. Seung and D.R. Nelson, Phys. Rev. A **38**, 1005 (1988).
[12] A. Polyakov, Phys. Lett. **103B**, 207 (1981).
[13] M. Green, J. Schwarz, and E. Witten, *Superstring Theory* (Cambridge University Press, Cambridge, 1987).
[14] D.R. Nelson, in *Fluctuating Geometries in Statistical Mechanics and Field Theory*, edited by F. David, P. Ginsparg, and J. Zinn-Justin (Elsevier, Amsterdam, 1995).
[15] Jeong-Man Park and T.C. Lubensky, following paper, Phys Rev. E **53**, 2665 (1996).
[16] D.J. Amit, Y.Y. Goldschmidt, and G. Grinstein, J. Phys. A **13**, 585 (1980).
[17] Y. Choquet-Bruhat and C. DeWitt-Morette with M. Dillard-Bleick, *Analysis, Manifolds and Physics* (North-Holland, Amsterdam, 1982).
[18] B.A. Dubrovine, A.T. Fomenko, and S.P. Novikov, *Modern Geometry — Methods and Applications, Vol. 2*, (Springer-Verlag, Berlin, 1985).
[19] F. David, in *Proceedings of the V Jerusalem Winter School* (Ref. [1]).
[20] W. Helfrich, Z. Naturforsch. **28C**, 693 (1973).
[21] P. Canham, J. Theo. Biol. **26**, 61 (1970).
[22] V. Popov, *Functional Integrals in Quantum Field Theory and Statistical Physics* (Reidel, Dordrecht, 1983).
[23] W. Cai, T. Lubensky, T. Powers, and P. Nelson, J. Phys. II (France) **4**, 931 (1994).
[24] L. Peliti and J. Prost, J. Phys. (France) **50**, 1557 (1989).
[25] P. Nelson and T. Powers, J. Phys. II (France) **3**, 1535 (1993).
[26] See, for example, P. Chaikin and T.C. Lubensky, *Princi-*

ples of Condensed Matter Physics (Cambridge University Press, Cambridge, 1995).
[27] M. Spivak, *A Comprehensive Introduction of Differential Geometry* (Publish or Perish, Boston, 1979).
[28] M. Nakahara, *Geometry, Topology and Physics* (Adam Hilger, Bristol, 1990).
[29] A. Polyakov, *Gauge Fields and Strings* (Harwood Academic, Chur, 1987).
[30] J. Cardy, in *Phase Transitions and Critical Phenomena,* edited by C. Domb and J. Lebowitz (Academic, New York, 1986), Vol. 11.
[31] P.C. Martin, in *Probleme a N Corps., Many-Body Physics*, edited by C. DeWitt and R. Balian (Gordon and Breach, New York, 1968).
[32] J. Jose, L.P. Kadanoff, S. Kirkpatrick, and D.R. Nelson, Phys. Rev. B **16**, 1217 (1977).
[33] P.G. de Gennes and C. Taupin, J. Phys. Chem. **86**, 2294 (1982).
[34] J.M. Park and T.C. Lubensky, J. Phys. I (France) (to be published).

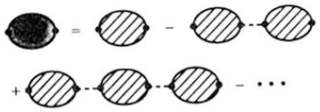

FIG. 5. Diagrammatic representation of the full $C^0_{\bar{n}\bar{n}}$ propagator when $\mathcal{H}_{nS} = 0$.

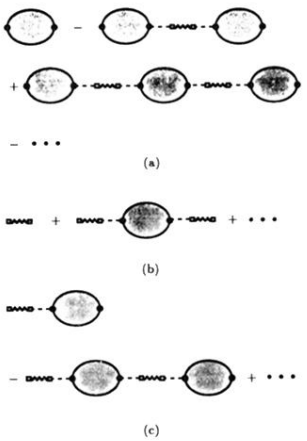

FIG. 7. Diagrammatic expansion of (a) $C_{\tilde{n}\tilde{n}}$, (b) $C_{\tilde{S}\tilde{S}}$, and (c) $C_{\tilde{n}\tilde{S}}$. The bubble is $C^0_{\tilde{n}\tilde{n}}$ represented in Fig. 5.